



Institute for Water
and Energy Sciences
(incl. Climate Change)



**PAN-AFRICAN UNIVERSITY
INSTITUTE FOR WATER AND ENERGY SCIENCES
(including CLIMATE CHANGE)**

Master Dissertation

Submitted in partial fulfilment of the requirements for the Master degree in
CLIMATE CHANGE ENGINEERING

Presented by

Christopher Padi Tuwor

TITLE:

**Estimating The Cooling Potential of Urban Green Spaces in Mitigating Urban
Heat in The City of Accra**

Defended on 14/04/2025 Before the Following Committee:


Chair	António Bento Gonçalves	Pr.	Affiliation (Institution only)
Supervisor	Anabella Ferral	Prof.	Affiliation (Institution only)
Co-supervisor	Giuliana Beltramone	Miss	Affiliation (Institution only)
External Examiner	Isaac Tchuwa	Dr.	Affiliation (Institution only)
Internal Examiner	Habi Mohammed	Dr.	Affiliation (Institution only)

DEDICATION

This work is dedicated to my beloved family, whose unwavering support and love have been my constant source of strength, including those dear members who, though no longer with us, continue to inspire me from beyond.

DECLARATION

I, **Christopher PADI TUWOR**, hereby affirm that the thesis presented herein is the result of my independent research, conducted to the fullest extent of my intellectual capacity and academic integrity. This thesis represents my own original work and has not been submitted, in whole or in part, for consideration for any other degree, diploma, or accolade in this or any other institution. Where collaboration has occurred, it has been explicitly recognized, and the contributions of others have been clearly identified and duly acknowledged. All sources of information, including published works and personal communications, have been referenced in accordance with scholarly standards. This declaration upholds my commitment to academic honesty and the advancement of knowledge within the framework of ethical research practices.

Signature: 

Date: 25TH March 2025

Master Christopher PADI TUWOR

Reg. No: 2023/MWE13

This thesis represents the original scholarly contribution of the candidate, developed under our supervision and guidance. It has been prepared in accordance with the academic standards required by our institution and is submitted for examination with our full endorsement as the candidate's appointed University Supervisors.

Signature: 

Date: 25TH March 2025

Prof. Anabella FERRAL

Institution: Instituto Gulich, UNC-CONAE

Signature: 

Date: 25TH March 2025

Miss Giuliana Beltramone

Institution: Instituto Gulich, UNC-CONAE

ACKNOWLEDGEMENT

I am profoundly grateful to the African Union Commission for their generous support in the form of a scholarship and research grant, which were instrumental in the realization of this research. My sincere appreciation also goes to all members of the Pan African University Institute of Water and Energy Sciences (PAUWES) for their invaluable contributions. A big thank you to the coordinator of the climate change program, for his support throughout the program. Special acknowledgement is reserved for the Director of PAUWES, whose wisdom has steered the institution to this height.

My deepest appreciation is extended to my esteemed research advisors, Prof. Anabella Ferral and Miss Giuliana. Their expert guidance, unwavering support, and insightful feedback have been pivotal in the completion of this research. The opportunity to work under their tutelage has been both an honour and a privilege, leaving an indelible mark on my professional and personal growth.

I am eternally grateful to my family, friends and colleagues for their endless love, prayers, and encouragement. Their belief in me has been a source of strength and motivation, reminding me of the importance of perseverance and resilience.

Finally, I extend my thanks to everyone who has played a part in this academic journey, both directly and indirectly. Your support, in all its forms, has been essential to the success of my research. This acknowledgment extends beyond words, embodying a profound sense of gratitude for the collective effort that has made this achievement possible.

TABLE OF CONTENTS

DEDICATION.....	i
DECLARATION.....	ii
ACKNOWLEDGEMENT.....	iii
LIST OF FIGURES.....	vi
LIST OF TABLES.....	vii
ABSTRACT.....	ix
1. INTRODUCTION.....	1
1.1. Background.....	1
1.2. Problem Statement.....	2
1.3. Research Objectives.....	2
Main Objective.....	2
1.3.1. Specific Objectives.....	3
1.4. Research Questions.....	3
1.5. Significance of the Study.....	3
2. LITERATURE REVIEW.....	5
2.1. Literature Review of Previous Studies.....	5
2.2. Overview of Climate Change.....	8
2.3. Climate Change Model.....	8
2.3.1. Climate Scenarios.....	9
2.3.2. Scenario Descriptions.....	9
3. RESEARCH DATA AND METHODOLOGY.....	11
3.1. Description of Study Area.....	11
3.1.1. Location.....	11
3.1.2. Climatology.....	12
3.2. Datasets.....	13
3.2.1. Satellite products (L8 L2C2).....	13
3.2.2. Land Cover/Land Use (LULC) Products.....	13
3.2.3. LULC: ESA Land Cover vs Dynamic World.....	14
3.3. Methodology.....	14
3.3.1. Methodological flow chart.....	15
3.4. Data Processing and Analysis.....	15
3.4.1. Description, Accuracy Assessment and Validation of LULCs.....	16
3.4.2. Computation of LST And NDVI.....	18
3.4.3. Spatial Analysis of LST and NDVI.....	22
3.4.4. Temporal Analysis of LST and NDVI.....	22

3.4.5. Zonal Statistics (LST and NDVI)	23
3.4.6. Determination of Cooling Potential of Green Spaces	24
3.4.7. Estimating the Cooling Potential Using Buffer Analysis	24
3.4.8. Correlation Between NDVI and LST	26
3.4.9. Scenarios	26
4. RESULTS AND DISCUSSION	28
4.1. LULC VALIDATION	28
4.1.1. Confusion Matrices	28
<i>Table 4. 1: PA, UA, Overall Classifications for ESA, 2021</i>	28
4.2. LST and NDVI.....	30
4.2.1 Spatio-Temporal Changes in LST and NDVI.....	30
4.2.2 Zonal Statistics: Varying LST and NDVI Across Various LULC	35
4.3. Cooling Potential of Green Spaces	38
4.4. Cooling Intensity of UGSs.....	39
4.4. Regression Analysis.....	40
4.5. Scenarios	41
4.5.1. Urbanization vs Greening	41
4.5.2. Shared Socio-economic Pathways	42
4.6. DISCUSSION	43
5. CONCLUSION AND RECOMMENDATION.....	45
5.1. Conclusion	45
5.2. Recommendation	46
6. REFERENCES	47

LIST OF FIGURES

Figure 3. 1: Map of the study area	20
Figure 3. 2: Methodological Flow	23
Figure 3. 3: Showing UGS and Buffer zones with 30 meter intervals	34
Figure 4.1: Showing the ESA World Class and DW 2021 classification maps of Greater Accra...	37
Figure 4.2: LST and NDVI for dry season in Accra, 2021	41
Figure 4.3: LST Trend Across Various Towns(2015-2024)	42
Figure 4.4: Monthly NDVI Trend in Accra with Change Point	42
Figure 4.5: LST and NDVI time series for dry season in Accra, (2015-2024)	43
Figure 4.6: Mean LST for dry season across various LULC, 2021	45
Figure 4.7: Mean LST for dry season across various LULC, 2021	46
Figure 4. 8: Showing Areas of Green and Non-Green Spaces	47
Figure 4. 9: Cooling Potential Across 30m Buffer Rings(per Park)	48
Figure 4. 10: Graph of LST and NDVI	49
Figure 4. 11: Figure showing the spatial changes in afforestation scenario against built-up	50
Figure 4. 12: Shared Socio-Economic Pathway	50

LIST OF TABLES

Table 3. 1:Description of Satellite data used in the study	22
Table 3. 2: Showing Various Classifications Under ESA World Cover and Dynamic World Map 2021, Accra	25
Table 3. 3: Details of formula used for LST calculation from Landsat level 1 data	29
Table 3.4: Showing description of each UGS	33
Table 4. 1: PA, UA, Overall Classifications for ESA, 2021	37
Table 4. 2: PA, UA, Overall classifications for DW, 2021	38
Table 4. 3: Statistics of Mean LST for Dry Seasons of 2015, 2021, and 2024	41
Table 4. 4: Statistics of Mean NDVI of Dry Seasons of 2015, 2021, and 2024	42
Table 4. 5: Mean, minimum and maximum LST for dry season across various LULC, 2021	44
Table 4. 6: Mean, minimum and maximum NDVI for dry season, 2021	45

LIST OF ABBREVIATIONS AND ACRONYMS

Abbreviations	Description
AGB	Above Ground Biomass
CCI	Climate Change Initiative
CRS	Coordinate Reference System
DJF	December-January-February
ESMs	Earth System Models
GBI	green and blue infrastructure
GCMs	General Circulation Models
IAMs	Integrated Assessment Models
IPCC	Intergovernmental Panel on Climate Change
LST	Reducing Land Surface Temperatures
LULC	Land Use Land Change
MODIS	Moderate Resolution Imaging Spectroradiometer
NDVI	Normalize Difference Vegetation Index
PA	Producer's accuracy
RCPs	Representative Concentration Pathways
SCP	Semi-automatic Classification Plugin
SSPs	Shared Economic Pathways
UGB	Urban Green Spaces
UHI	Urban Heat Island
USGS	U.S. Geological Survey
UTFVI	Urban Thermal Field Variance Index

ABSTRACT

The tropical region of Africa is noted for high temperatures which has implications for comfortable and quality life with consequential impact on human health. Urban green spaces (UGB) are efficient in mitigating urban heat but a compassing study to understand the role of vegetation in reducing Land Surface Temperatures (LST) in the city of Accra is lacking. This research estimates how much greenness can be utilized to reduce LST and prevent rising urban heat island (UHI) effect. This study is based on both spatial, temporal and statistical analysis of LST and NDVI. Spatial analysis of UHI revealed high LST in the coastal areas and lower LST in areas up north where vegetation cover is high. Across the 25-year period (2021 to 2024) LST showed an increasing trend and NDVI an inverse trend by employing Mann-Kendall Analysis. For the year 2015, 2021 and 2024 mean LST observed were 30.51°C, 35.60°C and 34.92°C respectively. Similarly, spatial results showed an equally spreading trend of LST values in major towns and cities, emphasizing the need for urban greening to reverse the trend. Peri-urban towns such as Dodowa and Big Ada showed lower LST compared to highly urbanised areas such as Nungua, La and Adabraka. Well planned areas such as Tema, Legon and East Legon showed moderate to low LST values. Trees had the highest NDVI and the lowest LST while built-up areas conversely showed the lowest NDVI and high LST respectively. Vegetated and non-vegetated areas showed a varied range of LST, with Mean LST in non-vegetation area being 37.30°C and vegetation 33.32°C, further bolstering the role of greens in reducing high temperatures. Using a simple regression model, a moderate but strong inverse relationship between LST and NDVI was observed, using 2021 data. The equation showed a Coefficient of Determination (R^2) of 0.57. The result suggests a strong influence of vegetation cover on LST, underscoring the need for afforestation, green roofing and urban parks in the region. Upon analysing the cooling potential of five urban green spaces, it was observed that two out of five have significant cooling potential. Legon Botanical Garden performed with a cooling potential of 4.1°C at 550m, followed by Achimota Forest at 3.3°C at the same distance. The weakest performer was the Efua Sutherland Childrens' Park due to its small size and the presence of a highly built surrounding. Scenario analysis revealed that converting 80% of grassland into areas with a minimum NDVI of 0.27 could result in at least a 1°C decrease in land surface temperature, based on 2021 Landsat data. It is therefore important that green spaces are maximisation in urban development.

1. INTRODUCTION

1.1. Background

The rapid expansion of urban areas has resulted in a significant increase in Urban Heat Island (UHI), a phenomenon where the city's land surface temperature (LST) is noticeably higher than its surrounding rural areas (Feyisa et al., 2014). UHI can be attributed to the widespread use of impervious surfaces such as concrete, pavements, and asphalts, which absorb, retain, and emit heat. Also, the size and form of urban areas have been proven to influence this effect (Zhou et al., 2017). In addition, the simultaneous reduction in green spaces, such as parks, street trees, forested pieces of land, and gardens, has contributed to the elevated temperatures being experienced in many cities in West Africa in recent times. Studies have shown that urban green spaces can significantly reduce surface temperatures by up to 2°C to 5°C compared to urban areas with minimal vegetation (Teferi & Abraha, 2017). The dynamics of urban heat in West Africa are hugely influenced by Land Use Land Change (LULC), seasonal variability, and recently, worsened by climate change. Between the period 1984 and 2016, 64.5% to 75.5% of green spaces were lost and this resulted in about 1 to 2 °C of temperature increase across the subregion (Owusu, 2018., Umar, n.d.). The average temperature in Accra has already been revealed to have risen above 1°C compared to the 1960s (Awuni et al., 2023). There is a strong positive correlation between the mean land surface temperature (LST) and the density of impervious surfaces and a negative correlation with green spaces (X. Li et al., 2013; Estoque et al., 2017). From 1990 to 2020 there has been significant urban forest cover loss due to an increase in built and cultivated areas within five metropolitan areas across Ghana (Oppong et al., 2023). Urbanization induced impacts are noted to be greater in humid climates, like Accra, than in arid regions (Li et al., 2023), a phenomenon that would be worsened by climate change (Andrade et al., 2023; Yang et al., 2023) if not addressed.

Rising temperatures worsen and amplify the urban heat island phenomenon and lead to more frequent heat waves with more hot days and fewer cold days (Global Climate Change, n.d; Intergovernmental Panel on Climate Change (IPCC), 2022; Shi et al., 2024). Exposure to extreme heat events has been shown to worsen various long-term health conditions, resulting in higher rates of illness and death (Liu et al., 2022). Other studies consistently show that individuals with mental illness have been found to experience more severe morbidity and mortality outcomes when exposed to high temperatures over a single day, in comparison to

those without mental illness (Meadows et al., 2024). It has also been shown by Damte et al, (2023) that climate change impacts, including rising temperatures, exacerbate prevailing health conditions in slum areas, and rise in cases of vector-borne diseases in cities. These perturbations caused by urban heat in the city are likely to increase, especially considering climate change scenarios induced by anthropogenic activities (Yang et al., 2023).

To mitigate urban heat, increase in the quantity and quality of urban green spaces (UGS) have proven to be an effective approach. To reduce UHI, ecosystem-based solutions such as the strategic use of natural elements, including green and blue infrastructure (GBI), create climate-resilient and adaptable urban environments. These solutions not only provide regulating services like temperature regulation but also offer additional benefits like stormwater regulation, air quality improvement, and recreational spaces. Moreover, green spaces can enhance air quality, decrease noise, and contribute to overall human health and well-being (Pinto et al., 2023). Consequently, it is essential for Accra to prioritize the incorporation of green spaces into urban planning and architectural designs (Aram et al., 2019). This will not only address the problem of increasing temperatures but contribute significantly to the long-term resilience and quality of life in the city. Integrating green spaces into urban development will reduce carbon emissions into the atmosphere and mitigate global warming and climate change (Oliveira et al., 2011). The amount of green space required to reduce urban heat in Accra is still yet to be researched.

1.2. Problem Statement

A study conducted in 2020 by Li et al in a similar tropical region found that the cooling effects of green spaces in urban areas were most pronounced during the hottest times of the day, this signifies the potential of green spaces to provide relief in urban areas experiencing extreme temperatures. However, the effectiveness of urban green spaces in cooling the environment in Accra, a rapidly urbanizing city, remains largely unexplored.

1.3. Research Objectives

Main Objective

The primary objective of this study is to estimate how much greenness can reduce LST by at least a degree in the Greater Accra Region of Ghana.

1.3.1. Specific Objectives

- To assess the best performing land cover data for studying LULC in the region.
- To assess the spatial and temporal changes in LST and NDVI across various land cover types.
- To perform a comparative assessment of temperature difference between green spaces and non-green spaces.
- To assess the risk of climate change on heat stress under various shared socioeconomic pathways.
- To make science backed recommendations for policy makers, urban planners and raise awareness on the implication of rising heat in our urban spaces.

1.4. Research Questions

- How do urban green spaces influence land surface temperature patterns in Greater Accra?
- What is the relationship between green spaces, NDVI and temperature in Greater Accra?
- How can the cooling potential of urban green spaces be quantified to mitigate urban heat in Greater Accra?
- What amount of green space is required to reduce urban land surface temperature by a degree Celsius in Greater Accra?
- How does heat pan out in the future under various climate change scenarios in the Greater Accra.
- What are the implications of the study findings for urban planners, city managers, and policymakers in Greater Accra?

1.5. Significance of the Study

This research seeks to assess the relationship between urban green spaces and temperature dynamics in Accra, utilizing remote sensing data, observed temperature data, and spatial analysis techniques. The main objective is to find the amount of greenness necessary to reduce LST by at least a degree Celsius. By evaluating the cooling potential of green spaces this study seeks to provide valuable insights for urban planners, city managers, and policymakers to

incorporate green infrastructure in efforts to mitigate urban heat and improve the liveability of Greater Accra.

2. LITERATURE REVIEW

2.1. Literature Review of Previous Studies

In recent years, the study of green spaces, and their contribution to reducing urban temperatures, and human comfort, have received enormous attention (Peeters et al., 2020; Shashua-Bar et al., 2011). In a 2018 study, inhabitants interviewed held the belief that the decrease in plant life within Accra raises liveability issues, particularly concerning ecosystem functionality, increased temperatures, and air quality (Owusu, 2018). Other studies have been primarily focused on the influence of urban trees in improving air quality through the trapping of particulate matter (Mandal et al., 2023). The importance of green spaces in combating the impact of climate change in urban areas has been emphasized in many studies in Ghana (Nero et al., 2017; N-yanbini, 2023). However, very little study has been carried out to give concrete evidence of Urban Heat Island in the City. Gyima et al (2023) estimated the trend of Land Surface Temperature (LST) and Land Use Land Cover (LULC) and explored the impact on health and economic risks for the Greater Accra Metropolitan Area (GAMA). They concluded that the city is trading green spaces for heated surfaces (Gyimah et al., 2023). In 2020, Wemegah et al., mapped out UHI and its spatial extent and determined its impact on urban life using the Urban Thermal Field Variance Index (UTFVI). However, none of these studies estimated how much green space could reduce urban temperature. To inform urban planners better and optimize green spaces, our study aims to quantify the cooling effect of Accra's urban green spaces and estimate the amount of green Above Ground Biomass (AGB) area that is necessary to reduce temperature by at least 1°C, reducing climate change vulnerability and extreme heat events.

Literature has established the relationship between green spaces and urban heat islands. The UHI effect created by the impact of sprawling urban growth can be mitigated through the utilization of green spaces as a promoter of the Cool Island Effect (Grilo et al., 2020) also known as Park Cooling Island (PCI). Contrary to UHI, the PCI is the phenomenon where the temperature is cooler within urban parks compared to that of surrounding areas. The PCI is a popular indicator that is used to characterize the cooling effect of urban green spaces on surrounding areas, with a strong correlation between PCI and air temperature (Chunming et al., 2024). Both UHI and PCI are key factors influencing the microclimate of urban areas.

Normalized Differential Vegetation Index (NDVI) can be used to assess and estimate the ecological value of green spaces and is most popular used to detect green cover by multispectral analysis of remote sensing data (Budiyanti, 2015; Huang et al., 2021). NDVI is a dimensionless index that quantifies the amount of vegetation cover and health based on the difference in reflectance between near-infrared and red light. NDVI also known as the ‘greenness index’ positively correlates with vegetation greenness, thickness, and health. It usually has an index value ranging between -1 and 1. The value 1 corresponds to areas completely covered by vegetation and intermediate values correspond to areas with weak or green cover such as water bodies, snow, concrete, sand, etc.

The rapid expansion of urban areas has resulted in a significant increase in Urban Heat Island (UHI), a phenomenon where the city’s land surface temperature (LST) is noticeably higher than its surrounding rural areas (Feyisa et al., 2014). UHI can be attributed to the widespread use of impervious surfaces such as concrete, pavements, and asphalts, which absorb, retain, and emit heat. Also, the size and form of urban areas have been proven to influence this effect (Zhou et al., 2017). In addition, the simultaneous reduction in green spaces, such as parks, street trees, forested pieces of land, and gardens, has contributed to the elevated temperatures being experienced in many cities in West Africa in recent times. Studies have shown that urban green spaces can significantly reduce surface temperatures by up to 2°C to 5°C compared to urban areas with minimal vegetation (Teferi & Abraha, 2017). The dynamics of urban heat in West Africa are hugely influenced by Land Use Land Change (LULC), seasonal variability, and recently, worsened by climate change. Between the period 1984 and 2016, 64.5% to 75.5% of green spaces were lost and this resulted in about 1 to 2 °C of temperature increase across the subregion (Owusu, 2018., Umar, n.d.). The average temperature in Accra has already been revealed to have risen above 1°C compared to the 1960s (Awuni et al., 2023). There is a strong positive correlation between the mean land surface temperature (LST) and the density of impervious surfaces and a negative correlation with green spaces (X. Li et al., 2013; Estoque et al., 2017). From 1990 to 2020 there has been significant urban forest cover loss due to an increase in built and cultivated areas within five metropolitan areas across Ghana (Oppong et al., 2023). Urbanization induced impacts are noted to be greater in humid climates, like Accra, than in arid regions (Li et al., 2023), a phenomenon that would be worsened by climate change (Andrade et al., 2023; Yang et al., 2023) if not addressed.

Increasing and optimizing green spaces in an ecosystem-based solution is one of the most effective measures to mitigate the urban heat effect. Green spaces can help to reduce the temperature of urban areas by providing shade, evapotranspiration, and a cooling breeze (Bowler et al., 2010). Ecosystem-based solutions for UHI involve the strategic use of natural elements, such as green and blue infrastructure (GBI), to create climate-resilient and adaptable urban environments. These solutions not only provide regulating services like temperature regulation but also offer additional benefits like stormwater regulation, air quality improvement, and recreational spaces. Moreover, green spaces can enhance air quality, decrease noise, and contribute to overall human health and well-being (Pinto et al., 2023). Consequently, it is essential for Accra to prioritize the incorporation of green spaces into urban planning and architectural designs (Aram et al., 2019). This will not only address the problem of increasing temperatures but contribute significantly to the long-term resilience and quality of life in the city. Integrating green spaces into urban development will reduce carbon emissions into the atmosphere and mitigate global warming and climate change (Oliveira et al., 2011). The amount of green space required to reduce urban heat in Accra is still yet to be researched.

AGB can be estimated using both direct and indirect methods. Direct methods to estimate AGB are based on field measurements, which sometimes result in destructive processes to determine the biomass of each sample. Indirect methods utilize remote sensing techniques and have proven to overcome the disadvantages of direct measurement (Kelsey & Neff, 2014; Zhu & Liu, 2015; López-Serrano et al., 2019). According to Alegria (Alegria, 2023) there is a good relationship between NDVI and AGB which allows for estimation of green spaces in urban areas. High values of NDVI and AGB indicate areas with dense vegetation cover.

This research seeks to assess the relationship between urban green spaces and temperature dynamics in the Greater Accra Region of Ghana, utilizing remote sensing data, observed temperature data, and spatial analysis techniques. Our main objective is to find the amount of green space necessary to reduce urban air temperature by a degree Celsius. By evaluating the cooling potential of green spaces this study seeks to provide valuable insights for urban planners, city managers, and policymakers to incorporate green infrastructure in efforts to mitigate urban heat and improve the liveability of Accra.

Urban green spaces such as parks, gardens and forest reservations are essential to maintaining sustainable cities as they act as shading and propagate evapotranspiration, both important processes that mitigate urban heat island effect (Borsah et al., 2025). To quantify the cooling

effect of green spaces, various researchers have employed remote sensing techniques, spatio-temporal analysis, and buffer analysis (Liu et al., 2022; Shi et al., 2024; Spronken-Smith & Oke, 1998). Buffer analysis involves creating concentric zones around the green space and measuring the change in LST at intermittent distances (Yu et al., 2017).

2.2. Overview of Climate Change

Climate change is expected to continue in an upward trajectory according to latest findings. Global warming, caused mainly by human activities through greenhouse gases emission, is expected to raise global surface temperatures further above 1.3 °C according to the latest Assessment Report (AR6). The year 2024 is the first on record to exceed 1.5°C above pre-industrial era, a threshold set by IPCC as part of the Paris Agreement (Bevacqua et al., 2025). This will spell out widespread and rapid changes in weather patterns and climatic conditions across the globe (Calvin et al., 2023).

The impact of these changes exposes over 3.6 billion people to multiple hazards. These highly vulnerable people continue to suffer from water and food insecurities, physical impact from extreme events such as floods, drought and storms, including extreme heat resulting in high human mortality (Tong et al., 2021). Key infrastructure, livelihoods, and human health have all suffered as a result of the observed climate change in metropolitan settings.

In urban areas, hot extremes have peaked. Extreme and slow-onset events have weakened urban infrastructure, such as transportation, water, sanitation, and electricity systems, leading to socio-economic losses, and detrimental effects on well-being. The negative effects that have been observed are concentrated among urban dwellers who are socially and economically marginalised (Hsu et al., 2021).

2.3. Climate Change Model

Climate change modelling refers to the scientific practice of creating computer-based simulations to understand and predict the behaviour of Earth's climate system under various scenarios, particularly those influenced by anthropogenic factors such as greenhouse gas emissions. This discipline has gained significant prominence in the context of global climate change, as it provides essential insights for policymakers, researchers, and the public regarding future climate conditions and potential mitigation strategies. The evolution of climate models—from early simplistic representations to today's sophisticated simulations—reflects the growing

urgency to address climate change impacts on ecosystems and human societies (O'Neill et al., 2014). The history of climate change modelling dates back to the mid-20th century when initial research laid the groundwork for more complex models. The introduction of powerful computers in the 1960s allowed scientists to transition from theoretical frameworks to practical simulations, resulting in General Circulation Models (GCMs) and Integrated Assessment Models (IAMs) that now underpin much of climate science. Modern climate models, including Earth System Models (ESMs), incorporate vast amounts of data and complex interactions among the atmosphere, oceans, and land, enabling researchers to project various climate scenarios based on historical trends and future emission trajectories.

2.3.1. Climate Scenarios

In the latest AR6, the Intergovernmental Panel on Climate Change (IPCC) of the UN analyses the results of climate models utilizing the Coupled Model Intercomparison Project Phase 6 6 (CMIP6), including representations of physical processes and higher resolutions in comparison to CMIP5 generation of climate models. One of the most significant changes is the use of Shared Economic Pathways (SSPs) which include socioeconomic factors, instead of the previous Representative Concentration Pathways (RCPs)(Calvin et al., 2023). This new framework provides detailed pathways of society in the 21st century in response to climate change with regard to economic, technological, social and geopolitical pathways conditions. These narratives can assist policy makers and the scientific community in anticipating development routes for economic metrics like population growth and per capita GDP, as well as for greenhouse gas (GHG) to enable mapping of hazards to their society in a comprehensive, integrated way (Moss et al., 2010).

The release of additional GHGs affects the atmosphere's level of radiative forcing (a metric which describes the change in the Earth's energy balance due to factors like greenhouse gases) and therefore the extent of global warming. SSP-based scenarios are referred to as SSPx-y, where 'SSPx' refers to the Shared Socioeconomic Pathway describing the socioeconomic trends underlying the scenarios, and 'y' refers to the level of radiative forcing (in watts per square metre, W/m² resulting from the scenario by the year 2100ⁱ (like in the RCP scenarios).

2.3.2. Scenario Descriptions

SSP1-/ RCP2.6: SSP1, known as the "Sustainability" or "Taking the Green Road" pathway, describes an increasingly sustainable world where global commons are preserved and the limits

of nature are respected. Here, the focus is more on human well-being than on economic growth and income inequalities between and within states are reduced. Consumption is oriented towards minimising material resource and energy usage. These efforts result in the net-zero CO₂ emissions target being reached by around 2075. The SSP1–2.6 scenario is associated with radiative forcing of 2.6 W/m² by 2100.

SSP2-/ RCP4.5: SSP2, also called the “Middle of the Road” or medium pathway, extrapolates the past and current global development into the future. Income trends in different countries diverge significantly. Though there is a certain degree of cooperation between states, it barely improves. Global population growth is moderate, levelling off in the second half of the century. Environmental systems are somewhat degraded. CO₂ emissions remain around current levels until 2050, then decline but fail to reach net zero by 2100.

SSP3-/ RCP7.0: SSP3, known as the “Regional Rivalry” or “A Rocky Road” pathway, sees a revival of nationalism and regional conflicts that push global issues into the background. Policies increasingly focus on questions of national and regional security. Over time, the gap widens between an internationally connected society that contributes to knowledge- and capital-intensive sectors of the global economy, and a fragmented collection of lower-income, poorly educated societies that work in a labour-intensive, low-tech economy. Investments in education and technological development decrease. Inequalities worsen. Some regions suffer drastic environmental damage and CO₂ emissions are expected to double by 2100 compared to 2015.

SSP5-/ RCP8.5: In SSP5, known as the “Fossil-Fuelled Development” or “Taking the Highway” pathway, global markets are increasingly integrated, leading to innovations and technological progress. This social and economic development, however, is based on an intensified exploitation of fossil fuel resources with a high percentage of coal use and the prevalence of energy-intensive lifestyles worldwide, leading CO₂ emissions to triple by 2075 compared to 2015.

As we circumvent the complexity of climate change, these scenarios will guide the science community and act as direction for policy formulation and decision-making.

3. RESEARCH DATA AND METHODOLOGY

3.1. Description of Study Area

3.1.1. Location

The study was conducted over the Greater Accra Region of Ghana. The choice of study was based on the fact that Accra, the nation's capital, most populated and industrialized city is located in this region of Ghana and the exact boundaries of the city keep changing with urban expansion. Accra is one of the fastest growing cities in Africa, according to the United Nations Human Settlements Programme (UN-Habitat) research 2022 report. The population of the region is estimated to be 5,455,692 in 2021 according to the Ghana Statistical Services. It has a high population density of 37522 persons per square mile, making it the smallest of the country's sixteen administrative regions (3,245 km²) and accounting for 1.4% of the total land mass. Map of study area is shown below in figure 3.1

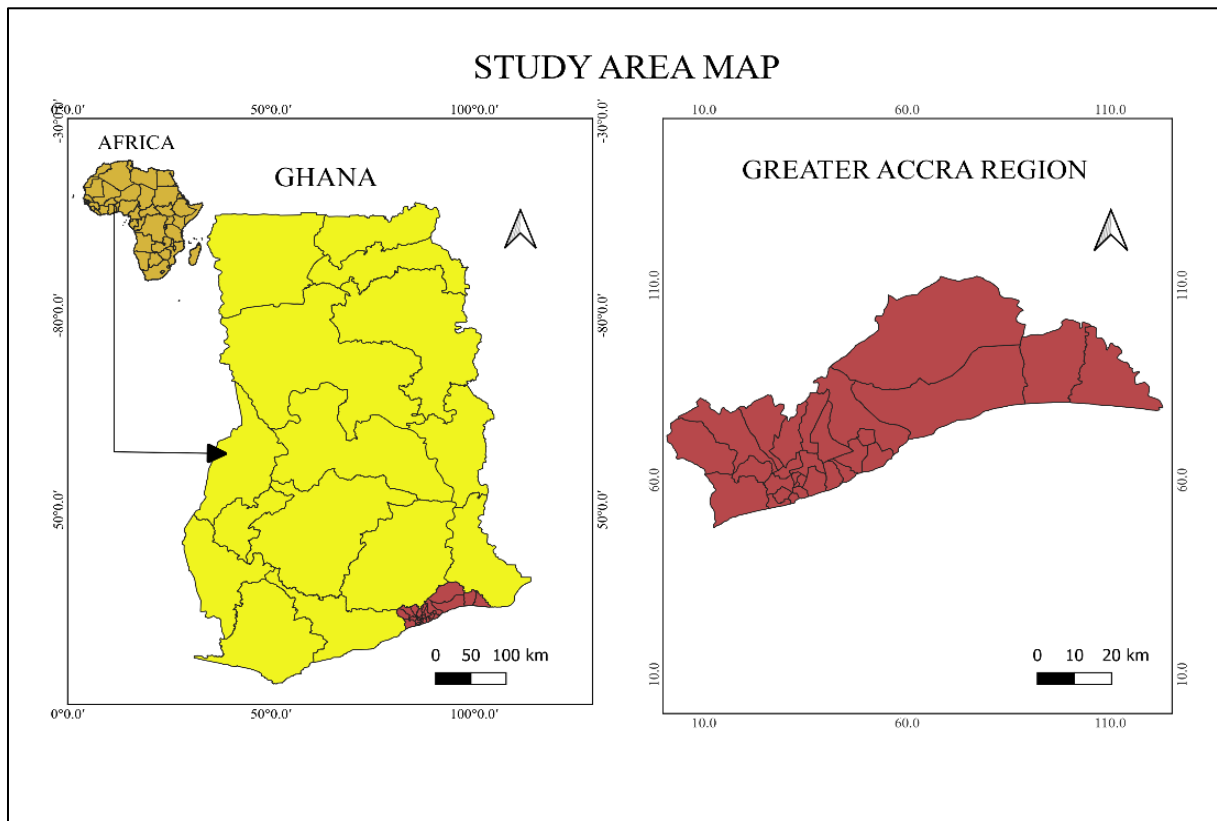


Figure 3.1: Map of the study area

3.1.2. Climatology

Accra is situated within the coastal savannah ecological and dry equatorial climatic zones (see Fig. 1). Positioned along the southern coast of the Gulf of Guinea, it is situated in the coastal area of Ghana, within the latitudinal boundaries of 5.5500 ° to 5.9167 °N and longitudinal boundaries of 0.2500 ° to 0.4167 °W. According to research, Accra faces the threat of climate change with rising temperatures, flooding and rising sea levels (Yazdanie et al., 2024). In 2023, Awuni et al found out that average temperature in the city had already risen above 1°C over the past four decades.

Climatologically, the average yearly temperature in the region is 25 °C, with mean monthly temperatures varying between 22 °C and 33 °C (Wemegah et al., 2020). According to the same study by Wemegah et al, February and March experience the highest temperatures, averaging around 24 °C to 33 °C, while June to September sees cooler temperatures with an average range of about 22 °C to 29 °C. Being within the coastal region of Ghana, which experiences a bimodal rainfall pattern, Accra major rainfall season starts from March to July. The minor season begins in September and ends in November. It records an average maximum rainfall amount of 420mm (Addi et al., 2021) The end of the coastal zone's rainy season occurs between the second and third ten-day periods of October, and the duration of the rainy season ranged from 210 to 220 days (Amekudzi et al., 2015). Then comes the dry season which begins usually from December till February (Osei et al., 2021). It is usually cloudy throughout the wet season with partial cloudiness during the dry season. Generally, Accra, on the east, is the driest part of the coastal region of Ghana (Bramah et al., 2021). The average yearly precipitation in the area under study ranges from 740 mm to 890 mm (Manzanas et al., 2014). The primary vegetation zones of Accra encompass coastal lands such as wetlands and dunes, as well as shrublands and grassland. It is generally a flat plan with very limited areas of higher elevation. LST is known to decrease with increasing elevation (Peng et al., 2020; Phan et al., 2018) and must be considered in any study but this will not be the case in our study area.

3.2. Datasets

The study utilized an array of data summarized in table 3.1

3.2.1. Satellite products (L8 L2C2)

Table 3.1: Description of Satellite Data used in the Study

Data	Spatial Resolution	Temporal Resolution	Source of Data
Landsat OLI/TIRS	8 30m	16 days	U.S. Geological Survey (USGS)
Landsat OLI/TIRS	9 30m	8 days	U.S. Geological Survey (USGS)
MOD11A2	1 km	8days composite	Moderate Resolution Imaging Spectroradiometer (MODIS)
MODIS/061/MOD13A2	1 km	16 days	Moderate Resolution Imaging Spectroradiometer (MODIS)
ESA World Cover	10m	annual	ESA Climate Change Initiative (CCI)
Dynamic World Land Cover Shapefile	World 10m	2-5 days	Google Earth Engine Humanitarian Data Exchange

3.2.2. Land Cover/Land Use (LULC) Products

ESA World Cover 2021 Map (v200) for the Greater Accra Region was obtained from the European Space Agency Website and delivered in 4 tiles as Cloud Optimized GeoTIFFs (COGs) in EPSG:4326 projection (geographic latitude/longitude CRS). The tiles were merged in QGIS and clipped to our study area. Classification Accuracy assessment was performed using Semi-automatic Classification Plugin (SCP) in QGIS and the output is shown in the table below.

Dynamic World Map 2021 for the Greater Accra Region was obtained from Google Earth Engine after signing up for its public data catalogue. The publicly available Java script was modified to incorporate our specific study area, duration and classification groups. Gray

GeoTIFFS was reclassified in QGIS and classification accuracy analysis was performed using SCP plugin. Map layout is shown in figure 3.2.

3.2.3. LULC: ESA Land Cover vs Dynamic World

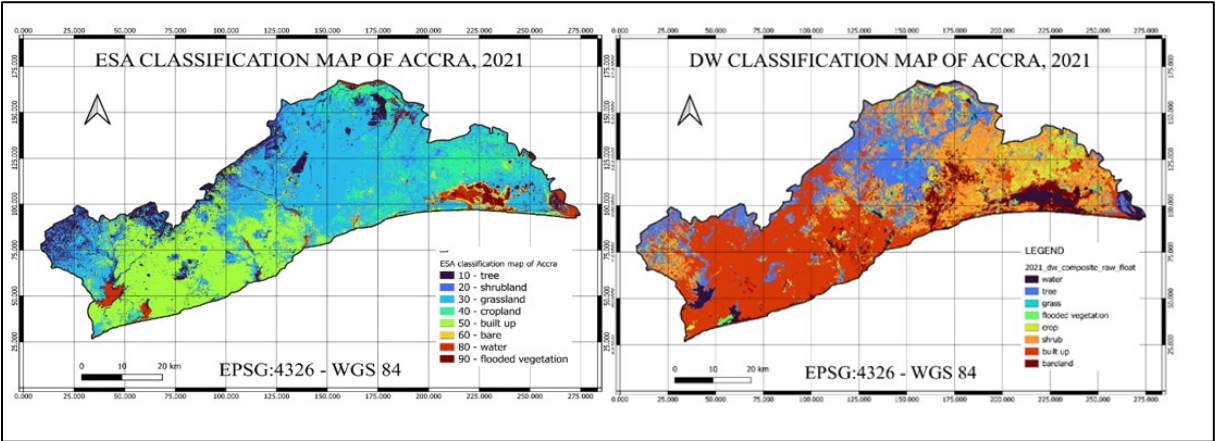


Figure 3.2: ESA World Class and DW 2021 classification maps of Greater Accra

3.3. Methodology

For this study, the overall workflow is divided into three tasks. The first task emphasizes the assessment of land cover data for the study area, calculation of LST and NDVI in QGIS and their variability across various land cover types. Spatial temporal evaluation of heat metrics and production of time series graphs followed. The last task is based on modelling the LST and NDVI relationship for the prediction of LULC using simple regression and building scenarios for LST reduction based on the relationship and scenarios of heat stress based on SSPs pathways using location risk intelligence tool.

3.3.1. Methodological flow chart

The figure (Figure 3.3) below describes the steps used in the analysis.

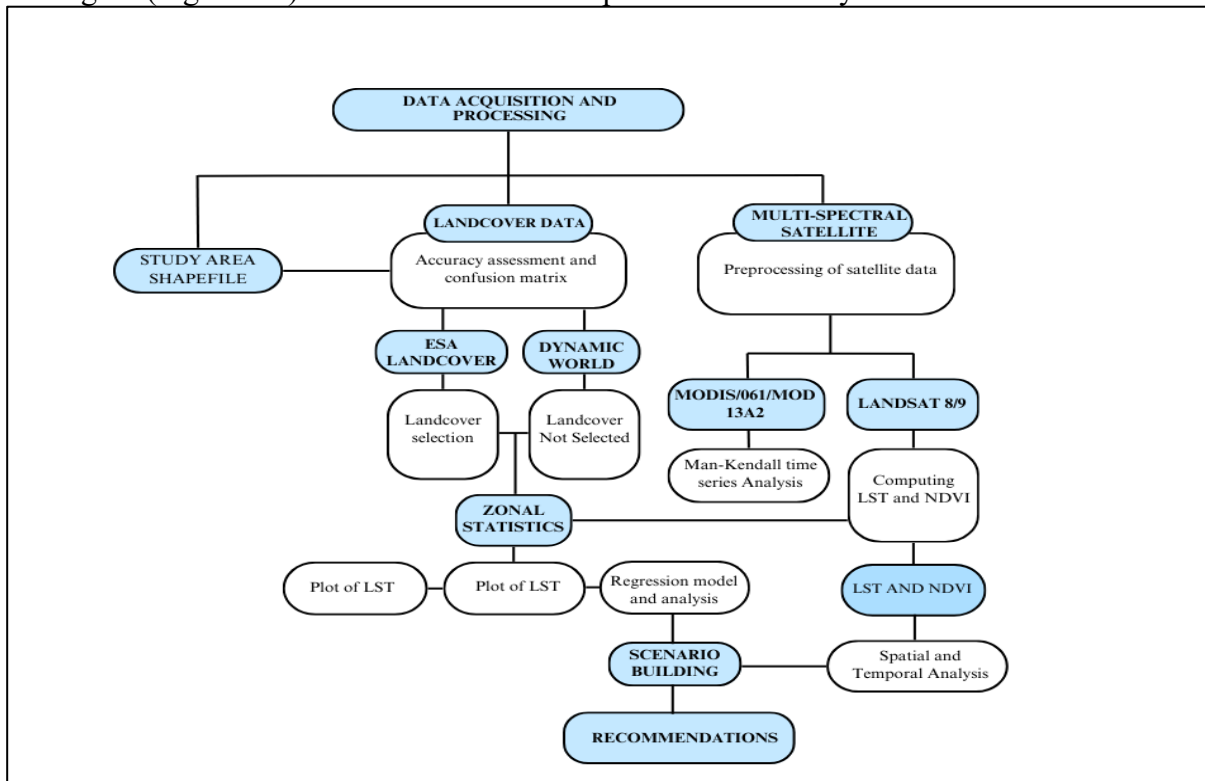


Figure 3.3: Methodological Flow

3.4. Data Processing and Analysis

In order to select the best dataset for our study, a quantitative comparative assessment was done to ascertain which LULC products most accurately classify our study area. This comparison was necessary given the number of publicly available LULC products (Duarte et al., 2023), where some products do underestimate or overestimate the real values of LULC in specific regions. For this study, two satellite data sets were considered for selection. These two data sets were chosen based on their ease of accessibility and no cost. Both datasets offer unique advantages and limitations, making it important to compare their spatial resolution, temporal frequency, data accuracy and specific characteristics that are relevant to study green spaces in the bustling city of Accra. Comparison between European Space Agency’s (ESA) World Cover map 2021 and Google’s Dynamic World 2021 was done to assess the accuracy of classification in order to select the best product for our study. The evaluation was done by calculating producer’s accuracy, user’s accuracy, and overall accuracy of these two products. Spatial Resolution of ESA World Cover Map and Dynamic World Maps

3.4.1. Description, Accuracy Assessment and Validation of LULCs

Description

The ESA World Cover Map has global land cover data. This high resolution provides a detailed insight into urban green spaces but may be limited in areas with highly fragmented classifications. Conversely, the Dynamic World Map relies on Google's advanced machine learning models providing real time land cover data with higher spatial scale of quality. This technology enhances the detection of smaller green spaces within densely populated urban areas. Below the main characteristics of both selected products are summarized.

- a. **ESA WORLD COVER 2021:** ESA World Cover Map 2021 at a 10-meter resolution is based on Sentinel-1 and Sentinel-2 constellations, provided over 10 land classes and delivered within the Coordinate Reference System (CRS) of regular latitude/longitude grid (EPSG:4326) with the ellipsoid WGS 1984. For the purposes of our study of the particular area the 8 classification groups (out of 11) were selected and shown in the table below (table 1). ESA World Cover Map is updated annually, making it ideal for long term studies but maybe limited for short term vegetation change monitoring.

- b. **DYNAMIC WORLD (DW) MAP:** Dynamic World 2021 is a near real-time dataset of 10m resolution global LULC provided by Google Earth Engine using its advanced deep learning algorithms. The Dynamic World Map is updated much more frequently, in some cases on a daily basis enabling a much more dynamic study of green space changes and assessing their cooling potential within different seasons. It covers 9 main classes based on Sentinel-2 satellite imagery shown in the table below (table 3).

Table 3.2: Showing Various Classifications Under ESA World Cover and Dynamic World Map 2021, Accra

Land Cover	CLASS NUMBER (ESA)	CLASS NUMBER (DW)	DESCRIPTION
Tree	10	1	Permanent waterbody including lakes, rivers and reservoirs
Shrub	20	2	Trees with a canopy cover greater than 10%
Grass	30	4	Shrubs and low-growing vegetation
Cropland	40	5	Grasses are the dominant vegetation, with few or no trees
Built up	50	6	Cultivated crops, including both annual and perennial crops
Bare	60	7	infrastructure such as buildings, roads, and other urban structures
Water	80	0	Land with little or no vegetation
Flooded vegetation	90	3	Vegetation is periodically or permanently submerged in water
Mangrove	95	8	Salt tolerant trees or shrubs that thrive mostly along the coastline where freshwater and sea meet.

Accuracy Assessment and Validation of LULCs

Accuracy assessment in the context of satellite image interpretation determines the quality of information derived from the remotely sensed data. The need for assessing the accuracy of any remotely generated map has become a universal practice in any classification research work (Olofsson et al., 2014). In order to carry out the assessment, we conducted various accuracies in percentages including the consumer accuracy, user's accuracy, overall accuracy and error matrix such as kappa coefficient. Our findings determine that the chosen remote sensing product for the study is fit for purpose (Morales-Barquero et al., 2019).

Formulas

Producer’s accuracy (PA) is defined as the probability that any pixel in that category has been correctly classified. This gives the accuracy of the map from the analyst’s point of view. This can be calculated using the formula as:

$$PA = \frac{\text{Total number of correct pixels in a category}}{\text{Total number of pixels of that category derived from the reference data(row total)}}$$

User’s accuracy (UA) is defined as the probability that a pixel classified on the image actually represents that category on the ground. This gives the accuracy of the map from the user’s point of view. It is calculated as given below:

$$UA = \frac{\text{Total number of correct pixels in a category}}{\text{Total number of pixels of that category derived from the reference data(column total)}}$$

Overall Accuracy (OA): It is also valuable to assess the overall accuracy of the classification across all classes present in the image. The overall accuracy metric provides a measure of the collective accuracy of the classification, quantifying the proportion of pixels that were correctly classified which is given below:

$$OA = \frac{\text{Sum of the diagonal elements}}{\text{Total number of accuracy sites (pixels)}}$$

3.4.2. Computation of LST And NDVI

Data Acquisition

Landsat8-9 OLI/TIRS C2 L2 data for the study area was taken during the dry season due to low cloud cover (Borsah et al., 2025) and the high intensity of LST during this season in Ghana (Twumasi et al., 2021). Furthermore, the dry season was chosen to exclude non-permanent green places that only exist during the wet season and to provide good classification results by reducing biases (Kwofie et al., 2022). The dry season for this study is chosen as December-January-February (DJF).

Vector data: The Accra vector file was downloaded from the official site of [Humanitarian Data Exchange](#) and used to crop satellite images.

Preprocessing LST and NDVI Data

The first step consists in masking clouds, heavy aerosols, and cloud shadows from each image. The resulting images are then clipped to the study area shapefile. The data was demarcated to

the spatial boundary of the study area. The map captures the spatial LST variations in Accra, with particular attention to key land cover and the seasonal period: the dry season (**December, January, February - DJF**) by filtering the data based on the seasonal timeframes and the average captured for the season. Due to the problem of cloud-coverage (Dissanayake et al., 2019; Estoque et al., 2017) especially during the wet season (AMJ), clouding masking was applied by using QA-PIXEL band to identify and mask cloudy pixels.

Previous studies have used various methods to calculate LST from Landsat8 Level 1 (LANDSAT/LC08/C02/T1_L1) data. They required LST by converting digital numbers (DNs) first into Top of Atmosphere (TOA) radiance, then into brightness Temperature at the top of the atmosphere and finally brightness temperature at the surface (atmospheric correction). The conversion of the DNs from thermal bands into absolute units of TOA radiance (J. Li et al., 2011; Weng, 2009) is done using equation (1).

$$L_{\lambda} = M_L Q_{CAL} + A_L \quad (1)$$

Where L_{λ} is TOA radiance (Watts/(m²*srad* μ m)); M_L is the band-specific multiplicative rescaling factor from the metadata; A_L represent the band-specific additive rescaling factor from the metadata; Q_{CAL} is Quantized and calibrated standard product pixel values (DN)(Twumasi et al., 2021).

Secondly, TOA radiance is converted to effective at-sensor brightness temperature assuming that the Earth's spectral emissivity is 1(Chander et al., 2009) i.e. as a black body, using equation (2).

$$T_b = \frac{K_2}{\left(\frac{K_1}{L_{\lambda}} + 1\right)} \quad (2)$$

where T_B is the effective at-sensor brightness temperature in degrees Kelvin, L_{λ} is the spectral radiance at the sensor's aperture in Watts/(m²*srad* μ m) and K_1 and K_2 are pre-launch calibration constants (Kwofie et al., 2022). Then, the bright temperature corrected by surface emissivity and atmosphere perturbation

To calculate LST, land surface emissivity (ε) was computed by using Equation (3).

$$\varepsilon = mP_v + n \quad (3)$$

where ε represents land surface emissivity; m represents $(\varepsilon_v - \varepsilon_s) - (1 - \varepsilon_s) F\varepsilon_v$; P_v represents the amount of vegetation; n represents $\varepsilon_s + (1 - \varepsilon_s) F\varepsilon_v$; ε_s is the soil emissivity; ε_v is the vegetation emissivity; and F is a shape factor whose mean value, assuming different geometrical distributions, is 0.55.

Land emissivity calculation: In this work we approximate emissivity using an NDVI derived approach (Mitraka et al., 2012) which allows us to estimate Proportion of vegetation. NDVI, calculated from the near-infrared (NIR) and visible red (VIR) spectrums, is obtained using the formula outlined in Table 3.1 as well as the proportion of vegetation (P_v).

Emissivity-corrected LST was calculated by using Equation (4) as follows:

$$LST = T_b / (1 + (\lambda \times T_b / \rho) \ln \varepsilon) \quad (4)$$

Where T_b is the at-satellite brightness temperature in degrees Kelvin; λ is the central band wavelength of emitted radiance (11.5 μ m for Band 6 and 10.8 μ m for Band 10 (Dissanayake et al., 2019)); ρ is $h \times c / \sigma$ (1.438 $\times 10^{-2}$ m K) with σ being the Boltzmann constant (1.38 $\times 10^{-23}$ J/K), h is Planck's constant (6.626 $\times 10^{-34}$ J·s), and c is the velocity of light (2.998 $\times 10^8$ m/s) (Dissanayake et al., 2019); and ε is the land surface emissivity estimated using Equation (3). Then, the calculated LST values (Kelvin) were converted to degrees Celsius ($^{\circ}$ C).

$$LST(^{\circ}C) = LST(K) - 273.15 \quad (5)$$

Where LST($^{\circ}$ C) is LST in Degree Celsius and LST(K) is LST in Kelvin.

For Landsat level 2 data, preprocessing is not required as these products have already undergone significant preprocessing (Chander et al., 2009). LST and NDVI calculations are carried out in QGIS using the raster calculator and the formulas below applied on specific bands.

$$LST = ("ST_B10" * 0.00341802) + 149.0 - 273.15 \quad (6)$$

Where ST_B10 is the Landsat 8 Thermal Infrared Sensor (TIRS) Band 10 data

0.00341802 = Radiance Multiplier factor for converting DN to TOA Radiance.

149.0 = Radiance Additive Factor (from Landsat metadata)

$$NDVI = ("B5" - "B4") / ("B5" + "B4") \quad (7)$$

Where B4 is band 4

B5 is band 5

Table 3.3: Details of formula used for LST calculation from Landsat level 1 data

Parameter	Formula	Description	Reference
Conversion of Digital Number (DN) to Top of Atmosphere (ToA) Spectral Radiance	$L_{\lambda} = M_L Q_{CAL} + A_L$	L_{λ} = Top of Atmosphere (TOA) spectral radiance (Watts/(m ² *srad*μm)); M_L =band-specific multiplicative rescaling factor from the metadata; A_L = band-specific additive rescaling factor from the metadata; Q_{CAL} is Quantized and calibrated standard product pixel values (DN)	(Twumasi et al., 2021)
Conversion of Spectral Radiance to Radiant Surface Temperature	$T_b = \frac{K_2}{\left(\frac{K_1}{L_{\lambda}} + 1\right)}$	T_B = effective at-sensor brightness temperature in degrees Kelvin, L_{λ} = spectral radiance at the sensor's aperture in Watts/(m ² *srad*μm) and K_1 and K_2 are pre-launch calibration constants.	(Kwofie et al., 2022)
NDVI	$NDVI = (R_{NIR} - R_{red}) / (R_{NIR} + R_{red})$	R_{NIR} = Band 5, Corrected near infrared band reflectance R_{red} = Band 4, Corrected red band reflectance	Sobrino et al. (2004)
Proportion of Vegetation	$P_v = [(NDVI - NDVI_{min}) / (NDVI_{max} - NDVI_{min})]^2$	$NDVI_{min}$ represents NDVI minimum value. $NDVI_{max}$ represents NDVI maximum value.	Sobrino et al. (2004)
land surface emissivity (ϵ)	$\epsilon = mP_v + n$	ϵ represents land surface emissivity; $m = (\epsilon_v - \epsilon_s) - (1 - \epsilon_s) F\epsilon_v$; P_v represents the amount of vegetation; n represents $\epsilon_s + (1 - \epsilon_s) F\epsilon_v$; ϵ_s is the soil emissivity; ϵ_v is the vegetation emissivity; and F is a shape factor whose mean value, assuming different geometrical distributions, is 0.55.	(Sekertekin & Bonafoni, 2020)

LST in Celsius	$LST = (T_b / 1 + (\lambda \times T_b / \rho) \ln \epsilon) - 273$	where T_b is the at-satellite brightness temperature in degrees Kelvin; λ is the central band wavelength of emitted radiance (11.5 μ m for Band 6 and 10.8 μ m for Band 10 (Dissanayake et al., 2019); ρ is $h \times c / \sigma$ (1.438×10^{-2} m K) with σ being the Boltzmann constant (1.38×10^{-23} J/K), h is Planck's constant (6.626×10^{-34} J·s), and c is the velocity of light (2.998×10^8 m/s)	(Dissanayake et al., 2019)
LST (using Level 2 Landsat data)	$LST = ("ST_B10" * 0.00341802) + 149.0 - 273.15$	where ST_B10 is the Landsat 8 Thermal Infrared Sensor (TIRS) Band 10 data 0.00341802 = Radiance Multiplier factor for converting DN to TOA Radiance. 149.0 = Radiance Additive Factor (from Landsat metadata)	(Jimenez-Munoz et al., 2014)

3.4.3. Spatial Analysis of LST and NDVI

Thermal data were obtained from USGS using merged Landsat 8/9 for the dry season for the years 2015, 2021 and 2024. The exact dates of data acquisition are 04/01/2015, 22/12/2021 and 22/12/2024 respectively. To obtain LST and NDVI values, formulas outlined in Table 2.4 were used. The LST and NDVI output for 2015, 2021 and 2024 are visualized in QGIS. To show better spatial comparison, the same scales, 10 and 50 respectively, were ascribed to minimum and maximum values for LST and -0.20 and 0.5 for NDVI in the QGIS visualization procedure. The quantile classification method and spectral colour ramp are applied to obtain proper urban heat visualization for LST. For NDVI, viridis colour ramp was chosen.

3.4.4. Temporal Analysis of LST and NDVI

To completely understand the changing dynamics of LST with respect to NDVI, a Mann Kendall time series analysis is performed for the period 2001 to 2021, a 21-year period. The Mann-Kendall trend test is a non-parametric statistical method used to detect trends in time series data, such as environmental data like temperature, rainfall, or vegetation indices (Yang et al., 2021; Zhang et al., 2022). This study utilized MOD11A2.061 Terra Land Surface Temperature and Emissivity 8-Day Global for LST and MOD13A2.061 Terra Vegetation

Indices 16-Day Global 1km data clipped and filtered for the study area and temporal period. This dataset is used because it is provided every 8 - 16 days at 1-kilometer spatial resolution as a gridded level-3 product in the Sinusoidal projection. The test relies on time series data, and MODIS' availability of multi-year, consistent satellite observations make it suitable for this type of analysis in tropics.

Mann Kendall test is applied to both indices to find the trend, statistical significance, the rate of change and change points.

3.4.5. Zonal Statistics (LST and NDVI)

Zonal statistics was performed in GEE to obtain LST values across the differing LULC classes and the result is summarized in table 3. ESA land cover and Landsat data obtained from USGS were uploaded in GEE. Nine different classes namely; Tree, Shrub, Grass, Cropland, Built-up, Bre, Water, Flooded vegetation and Mangrove are considered in this study. While previous studies (Frimpong et al., 2023; Gyile et al., 2025; Mantey et al., n.d.) considered fewer classes, in this study, it was desired to have a better understanding of LST distribution across all the LULC classes across the Greater Accra Region of Ghana.

Zonal statistics was performed in GEE to obtain NDVI across the differing LULC classes and the result is summarized in table 3.1. Nine different classes namely; Tree, Shrub, Grass, Cropland, Built-up, Bre, Water, Flooded vegetation and Mangrove are considered in this study. While previous studies considered fewer classes, in this study, it was desired to have a better understanding of LST distribution across all the LULC classes across the Greater Accra Region of Ghana.

The Normalized Difference Vegetation Index (NDVI) is a widely-used metric for quantifying vegetation health and density using remote sensing data (Wang et al., 2021). It is calculated using the following formula: $NDVI = (NIR - RED) / (NIR + RED)$ (Huang et al., 2021). NDVI values are sensitive to certain types and amounts of vegetation within various buffer zones, and increments in mean NDVI exposure values can be associated with changes in total greenspace percentage and individual vegetation types (Martinez & Labib, 2023). NDVI values range from -1 to +1. Higher positive values indicate healthier, denser vegetation. Values near zero suggest bare soil or no vegetation. Negative values often indicate water bodies (Huang et al., 2021).

3.4.6. Determination of Cooling Potential of Green Spaces

To determine the cooling potential of urban green spaces, the study area was reclassified into vegetative and non-vegetative areas GEE and visualized in QGIS. Due to low range of NDVI in Accra during the dry season, stratification method for multiple thresholds of NDVI was not reliable. Stow et al used NDVI value to classify vegetation, where vegetation = (NDVI > 0.2) and non-vegetation = (NDVI < 0.2) in Accra (Stow et al., 2013). Considering the high level of dryness during the study period, this study used a threshold of NDVI ≥ 0.20 to encompass enough vegetation cover. To calculate the cooling potential the formula below was utilized.

$$\text{Cooling Potential} = (\text{Mean LST in Non-Green Spaces}) - (\text{Mean LST in Green Spaces})$$

This formula has been widely used in similar studies even though it simplifies complex interactions (Kabisch et al., 2023).

3.4.7. Estimating the Cooling Potential Using Buffer Analysis

For this research we employed the buffer analysis approach to estimate the cooling potential of five urban spaces in Accra as this is cost effective and is devoid of human errors as could be the case in using in-situ measurements. It has been established that LST increases with each moving distance from the boundaries of green spaces (Spronken-Smith & Oke, 1998). These cooling effects have been proven to be significant up to 500m depending on the size of the green space under consideration (Chang et al., 2007).

Manually, UGS patches were selected using Google Earth. Due to the presence of irregular green space across the city, only green space patches with dense trees were considered as dense trees are known to have strong cooling effects. The selection process considered the following rules: green space must be covered primarily by trees, and green spaces must be devoid of water bodies and must be at least 300 m away from other green spaces or water bodies to avoid interference(L. Li et al., 2023). Based on these rules, five green spaces were selected. These are Achimota Forest, Legon Botanical Garden, Efua Sutherland Childrens' Park, Awudome and Osu Cemeteries. The size of each UGS is summarized in the table below (table 3.4).

Table 3.4: Showing description of each UGS

UGS	Area(ha)
Achimota Forest	464.98
Awudome Cemetery	30.72
Efua Sutherland Children’s Park	7.37
Legon Botanical Garden	80.92
Osu Cemetery	11.89

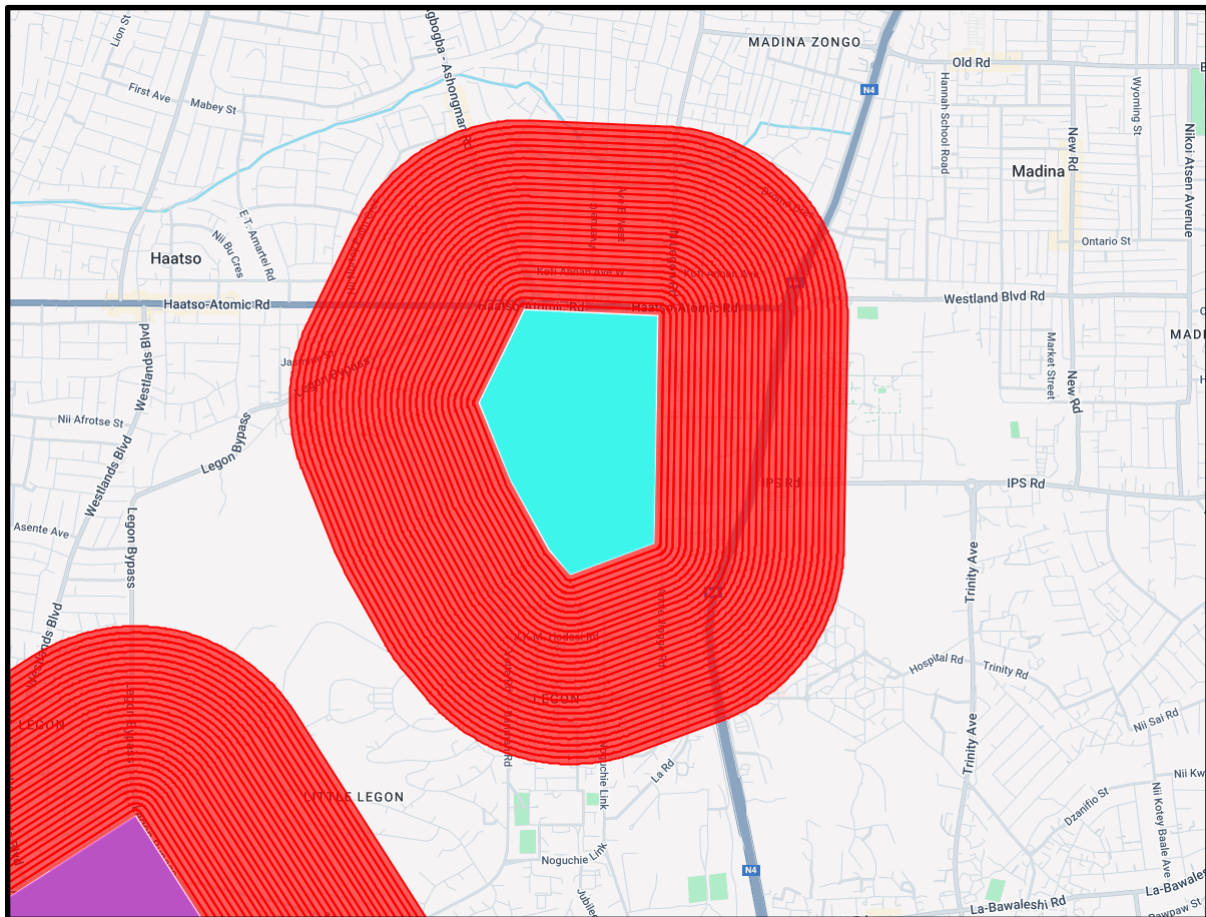


Figure 3.4: Showing UGS and Buffer zones with 30-meter intervals

Buffers of regular 30m intervals are created up to 600m based on previous studies (Peng et al., 2021; Yao et al., 2022) and mean LST is calculated within each buffer. Thirty metres was chosen due to the spatial resolution of Landsat 8 OLI as done in previous studies (Zhang et al., 2024). To compute the cooling potential, a difference of LST within the park and with each buffer zone is taken. It is expected that the cooling intensity will reduce with each increasing buffer distance. The distance where this cooling intensity diminishes or LST flattens is known as the cooling range. This is determined by the Cubic polynomial fitting with equation $y = ar^3 +$

$br^2 + cr + d$ (Zhang et al., 2024). The cooling intensity for each UGS is plotted against each interval.

3.4.8. Correlation Between NDVI and LST

To ascertain the relationship between NDVI and LST, QGIS was used to create joint points for NDVI and LST data. Four million points were generated using the nearest point method. This large number was downsized by 25% to 1,048,576 points using random selection. This was then exported as csv and in regression analysis was performed in python (Google Collab).

3.4.9. Scenarios

Deforestation (Built-up) and Afforestation

The rate of deforestation in Ghana is particularly of great concern. At the national level the rate of deforestation has been 3.5% annually (320,803 ha/year) since 2000(Adom et al., 2024). Using this rate of change, we applied the changes to the NDVI map by replacing 80% of grassland pixels based on ESA LULC data under two scenarios and applied the regression model to predict a new LST and visualised it in QGIS. This 80% of grass land cover represents 35 % of the total area of Greater Accra that would be changed in ten years according to the deforestation rate (Adom et al., 2024). The first scenario is considered as urbanisation where grassland area turned to built-up areas. Here 80 percent of grassland NDVI pixels were replaced by mean NDVI of trees (0.12), *see table 4.2*, in Google Earth Engine, turning 80 percent of grassland to built-up. The second scenario is afforestation by turning grassland into an area with trees. Here, 80 percent of grassland pixels were replaced by mean NDVI (0.27), *see table 4.2*, of tree class and a new LST was predicted using the same regression model in Google Earth Engine and Visualized in QGIS.

Urban Heat Index

Increasing global warming will lead to more incidents of urban heat and more heatwaves as projected by models (Perkins-Kirkpatrick & Lewis, 2020). As part of the analysis, urban heat index under various SSPs is examined using Location Risk Intelligence tool by Risk Management Partners.

Heat stress index is a quantitative measure that combines several factors related to temperature such as air temperature and relative humidity to assess the impact of heat on the human body

and comfort (Lanzante, 2024). The heat stress index classifies climatological heat stress situations on a scale ranging from 0 (very low) to 10 (very high).

4. RESULTS AND DISCUSSION

4.1. LULC VALIDATION

Producer's Accuracy represents the probability that a pixel from a specific class is correctly classified. PA values for ESA World Class Map range from 90.3478% to 100%. PA values of 100% suggest that all pixels from these classes were correctly classified by the model. Classes with PA values less than 100%, such as class 60 (bare land) with 90.3478%, may have some level of confusion with other classes, though they still performed well. All classes were classified with above 90% and half of these classes achieved 100% PA values. This indicated good performance of the data. For Dynamic World Map, PA values ranged 0 to 90.0648% with five classes showing PA values below 50%. This shows that while classification was good for a few classes, it failed to classify most of the classification groups.

User's Accuracy measures the probability that a pixel classified as a certain class actually belongs to that class. UA values for ESA World Class Map range from 98.4056% to 100%. Classes with 100% UA show no misclassification among those identified as belonging to that class. The class that shows a UA of 98.4056%, indicates some degree of misclassification, where the model incorrectly labels pixels as belonging to this class when they do not. This mishap is rather too small. For Dynamic World, UA values ranged between 0 to 99.6837% with one nan value indicating misclassification in the dataset. Nearly half of the classifications were below 50% user's accuracy.

The overall accuracy provides a summary metric, indicating the percentage of all correctly classified pixels. The result showed overall accuracy of 99.85% for ESA World Class Map meaning the classification appears to be almost perfect overall, suggesting that the model performed exceptionally well in correctly classifying almost all pixels across all classes, much better than the 70.96% performance Dynamic World Map.

4.1.1. Confusion Matrices

Table 4. 1: PA, UA, Overall Classifications for ESA, 2021

ERROR MATRIX										
ESA WORLD COVER	V_Classified	tree	shrub	grass	crop	built	bare	water	flooded vegetation	Total
tree	10	35546	0	0	0	3	0	0	0	35549
shrub	20	0	5685	0	62	0	0	0	0	5747
grass	30	0	0	11295	72	0	111	0	0	11478
crop	40	0	0	0	3204	0	0	0	0	3204
built	50	0	0	0	0	71225	0	0	0	71225
bare	60	0	0	0	0	0	1039	0	0	1039
water	80	0	0	0	0	0	0	2614	0	2614
flooded vegetation	90	0	0	0	0	0	0	0	1032	1032
Total		35546	5685	11295	3338	71228	1150	2614	1032	16471
PA [%]		100	100	100	95.98	99.995	90.3	100	100	
UA [%]		99.99	98.92	98.40	100	100	100	100	100	

Overall accuracy [%] = 99.8494
PA = producer's accuracy
UA = user's accuracy

Table 4.2: PA, UA, Overall classifications for DW, 2021

		ERROR MATRIX								
DYNAMIC		tree	shrub	grass	crop	built	bare	water	flooded	vegetation
WORLD	V_Clas	0	1	2	3	4	5	6	7	Total
	sified									
tree	0	0	1	0	4102	0	50	0	52	4205
shrub	1	0	25842	3985	2670	2596	691	0	0	35784
grass	2	0	0	0	55	117	0	0	0	172
crop	3	0	0	91	1534	0	6	0	0	1631
built	4	0	4551	13	111	47	884	0	0	5606
bare	5	0	216	795	0	6830	1196	0	4	9041
water	6	0	7	5	0	54	0	55153	109	55328
flooded	7	0	0	0	404	66	60	6084	815	7429
vegetation										
	Total	0	30617	4889	8876	9710	2887	61237	980	11919
	PA [%]	nan	84.4041	0	17.282	0.484	41.427	90.0648	83.1633	6
	UA	0	72.2166	0	94.052	0.8384	13.228	99.6837	10.9705	
	[%]				7		6			

Overall accuracy [%] = 70.9646
PA = producer's accuracy
UA = user's accuracy

4.2. LST and NDVI

4.2.1 Spatio-Temporal Changes in LST and NDVI

From the visual representation it can be seen that both LST and NDVI changed significantly over the years. LST increased generally across the region from 2015 to 2021. More specifically, the intensity of LST shifted more towards the east part of the region around towns such as Big Ada. The western portion shows significant reduction in LST especially all areas from Weija, to Tema and to Prampram, between 2015 and 2021. Areas in the western half, particularly around Big Ada show increased intensity in LST for the same period. However, towards 2024, LST intensity reduced marginally for the western portion and shifted slightly northward and increased significantly around Prampram.

NDVI declined spatially with many areas showing receding vegetation cover between 2015 and 2024. This decline is northward where vegetation cover is predominantly higher than in coastal areas. In 2021, some portions show improved NDVI, particularly all areas north of Prampram. Improved NDVI in some of these areas can partly be associated with the long period of locked down during the COVID-19 pandemic which limited anthropogenic activities (Andrade et al., 2023; Guha & Govil, 2021).

The line graph depicts a decade trend in mean LST across 15 known towns in the Greater Accra Region. The data reveals a dynamic landscape of heat variation that reflects both natural climate variability and human-induced LULC. The period 2015-2017 showed moderate LST mostly within 34°C–40°C while 2018 showed a rather cooling period in most towns with Accra, La and East Legon showing mean LST below 30°C. From 2019 to 2023, it was observed that many towns, such as Big Ada, Dodowa and Legon, had dips in mean LST. The year 2024 has seen a rebound in mean LST in nearly all towns. Worst performers are Prampram (44.10°C), Nungua (42.80°C), La (42.03°C). East Legon(22.04°C), Tema(29.18°C), and Legon(32.04°C) proved better performers with lower mean LST. Accra, Tema and Legon consistently showed moderate mean LST, reflecting their already well-planned neighbourhoods with patches of green spaces compared Weija and Adenta both which peaked at 45°C in 2023 suggesting intensified heating due to continuous loss in vegetation and increase in impervious surfaces (Awotwi et al., 2019). It is evident that towns with peri-urban nature such as Big Ada and Dodowa had lowered UHI compared to urban areas such as Nungua, La and Adabraka. (Adyatma et al., 2022; Agan, 2021). The rise in 2024 mean LST across board emphasises the relevance of the study.

The results show a statistically significant decreasing trend in NDVI values in Accra over the period, with a Mann-Kendall test p-value of 0.00268. The Pettitt test identifies a statistically significant change point around 2008(31-12-2008) with a comparatively higher confidence. The p-value of 0.0287 is less than 0.05, confirming the statistical significance of the detected change point. This suggests a more abrupt shift in the mean NDVI around late 2008.

On the contrary, an increasing trend in Land Surface Temperature (LST) in Accra is observed over the same study period (2015–2024), with a Mann-Kendall test p-value of 0.0359. The estimated rate of change is 0.0056°C per year, and Pettitt's test detects a potential change point around August 2012 (31-08-2012). From the result, the change point is August 2012 though

this was not statistically significant (p-value of 0.1776 is greater than 0.05) and therefore we cannot say with confidence that there was an abrupt change in LST around the period. The graph shows this change clearly as shown in figure 4.3.

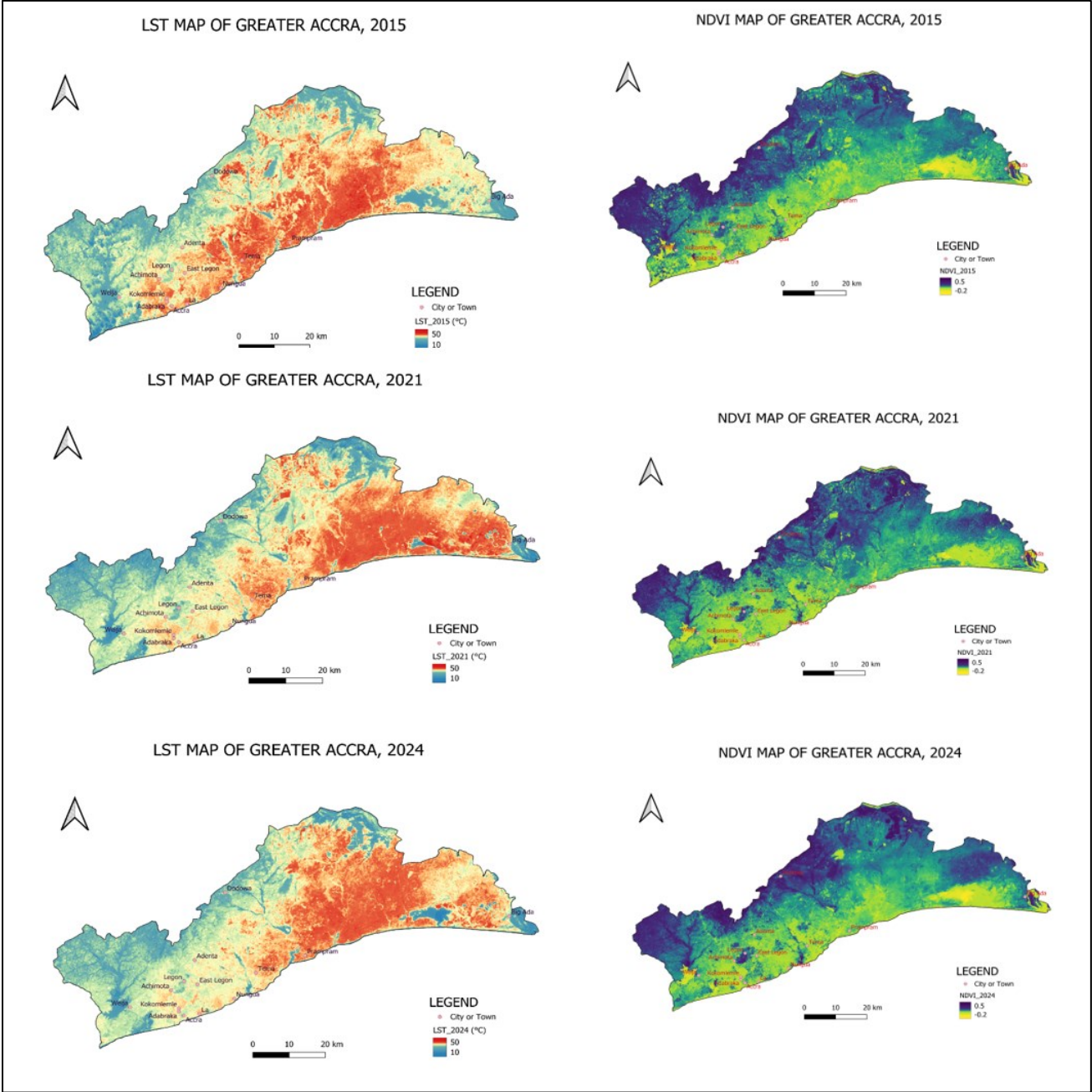


Figure 4. 1: LST and NDVI for dry season in Accra, 2021

Table 4.3: Statistics of Mean LST for Dry Seasons of 2015, 2021, and 2024

LST (°C)	2015	2021	2024
mean	35.86	35.83	36.42

Table 4. 4: Statistics of Mean NDVI of Dry Seasons of 2015, 2021, and 2024

NDVI	2015	2021	2024
mean	0.15	0.18	0.14

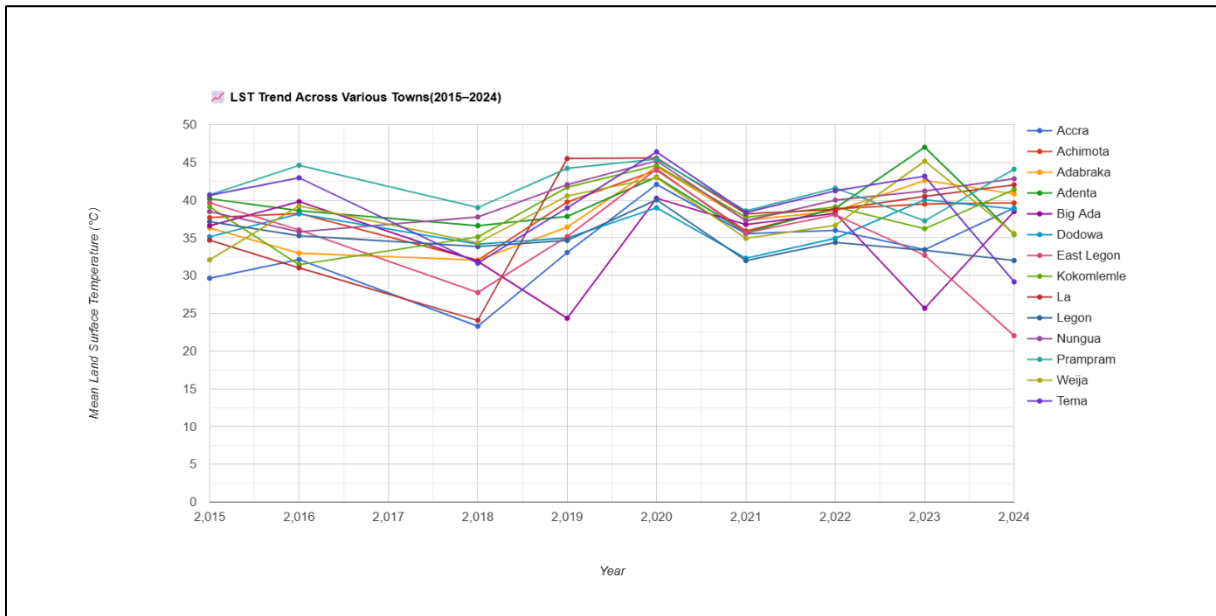


Figure 4.2: List Trend Across Various Towns (2015-2024)

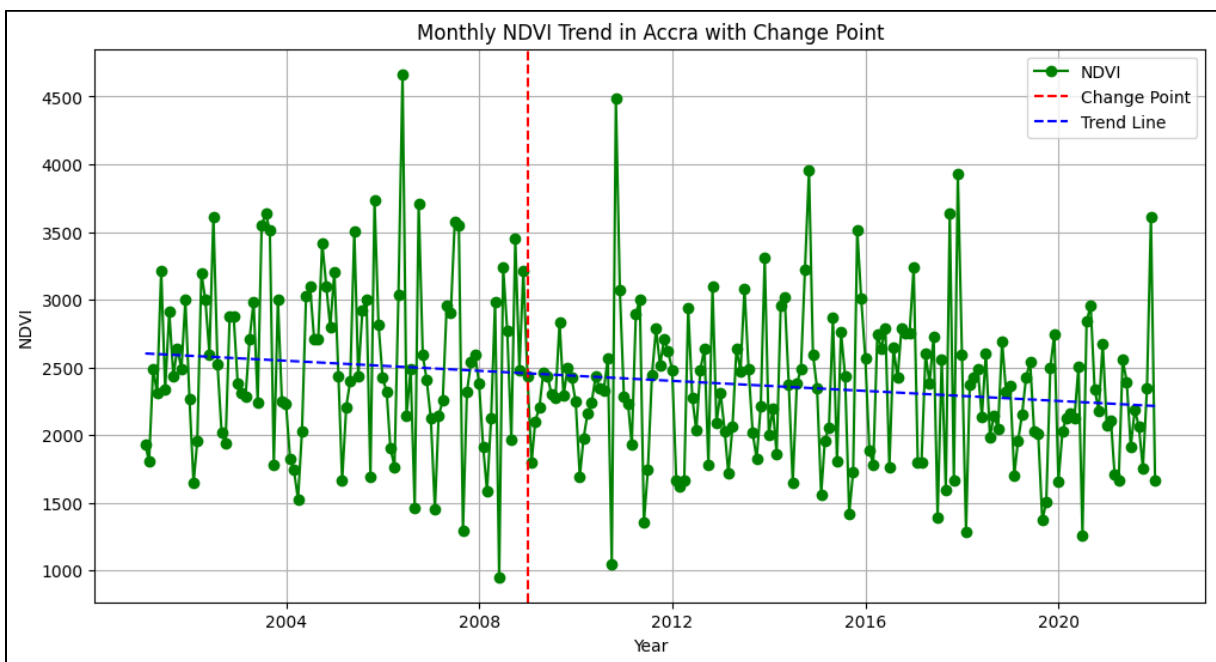


Figure 4.3: Monthly NDVI Trend in Accra with Change Point

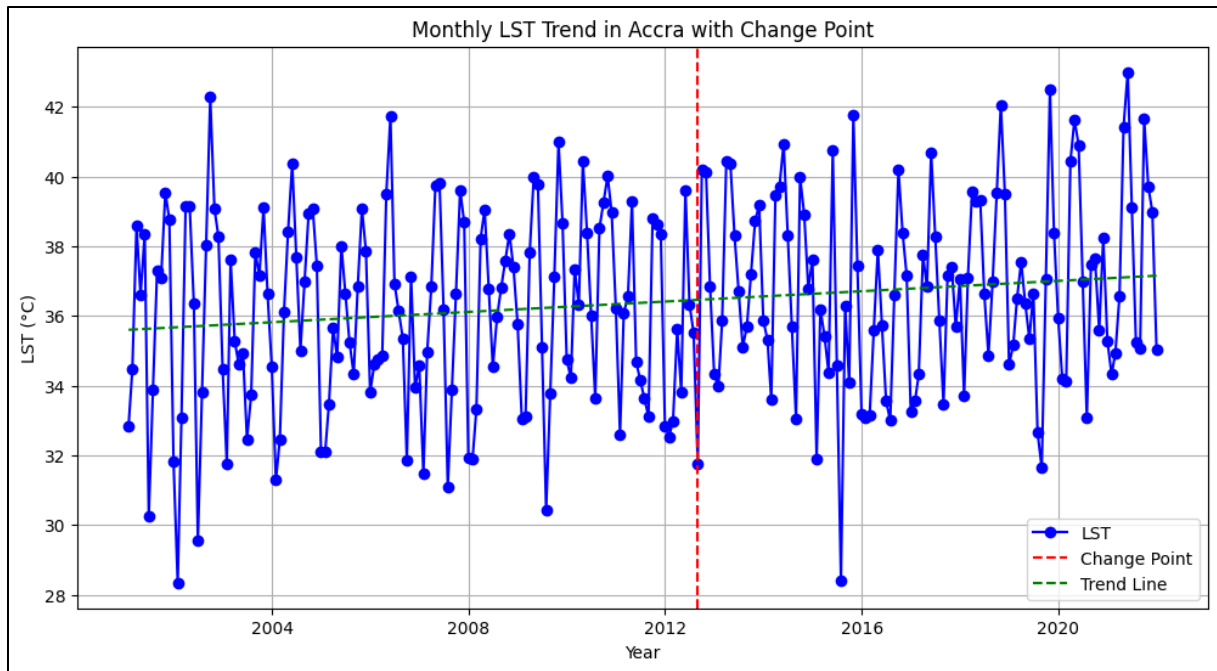


Figure 4.4: LST and NDVI time series for dry season in Accra, (2015-2024)

4.2.2 Zonal Statistics: Varying LST and NDVI Across Various LULC

The minimum values provide insight into cooler temperature distributions across the same land cover classes. Minimum LST values generally range from approximately 16.47°C to 26.20°C. Water recorded the lowest minimum LST and bare area with the highest.

Maximum LST ranged from 40.06°C to 49.41°C representing Mangrove and Built-up respectively. Mangrove has been proven to have a low LST due to high NDVI values compared to bare or built-up areas (Kanjin & Alam, 2024; Rendana et al., 2023). The highest LST were recorded for areas with less vegetation or with high amounts of impervious surfaces (Adyatma et al., 2022), for example water, bare, and built-up which showed values 47.22°C, 47.76°C and 49.41°C respectively. Values from Built-up showed relatively low standard deviation indicating low variation in the distribution across the land cover type. This also means Built-up has thermal stability which indicates low cooling potential (Zhao et al., 2020). This is due to the UHI effect that tends to create a "dome" of elevated temperatures over urban areas, which can lead to a more uniform temperature distribution within the built environment (Gyasi-Addo, 2021).

Averagely, mangrove, trees and water, and shrub had reduced mean LST with 30.31°C, 30.42°C, 30.70°C, and 32.18°C respectively. The highest mean LST were recorded in bare, cropland, grass and built-up areas in that order. The highest mean LST was bare with 38.84°C. In 2021, Built-up area was 25% of the entire Greater Accra Region while Grass occupied 43%.

These two classes alone with low vegetation and corresponding high LST (Ahmed et al., 2020; Asare et al., 2024) make up more than half of the entire region.

In general, LST ranged from 16.47°C to 49.41°C representing trees and built-up area respectively. Built up recorded the highest LST for study area similar to a study by (Gyile et al., 2025). A similar study by (Twumasi et al., 2021) found that the LST temperature for Accra ranged from 21.10°C to 46.13°C in 2020 for the same study area.

NDVI measured in the dry season for Accra ranged from 0.43 to -0.14 representing maximum NDVI of trees and minimum NDVI of water. Vegetation types such as shrubs, cropland, grass and mangrove also indicate relatively high NDVI with mean values of 0.42, 0.19, 0.18 and 0.17 respectively. As expected, water, bare and built-up show very average to low NDVI mean values of 0.02, 0.08 and 0.12 respectively. As was mentioned before NDVI for clear water bodies should be negative but positive values can be observed for waters with high amounts of biomass or for mixed pixels that contain water and land (German et al, 2020).

Table 4. 5: Mean, minimum and maximum LST for dry season across various LULC, 2021

Land Cover	Dn	Max(°C)	Mean(°C)	Min(°C)	Area (%)	StdDev
Tree	10	42.46	30.42	16.47	7.38	2.41
Shrub	20	44.91	32.18	16.48	6.58	2.90
Grass	30	47.32	37.13	18.92	43.58	3.22
Cropland	40	44.51	37.61	23.90	10.02	3.97
Built-up	50	49.41	35.86	25.46	25.80	2.24
Bare	60	47.76	38.84	26.20	2.00	3.69
Water	80	47.22	30.70	24.69	2.25	5.58
Flooded vegetation	90	47.60	35.91	24.75	2.14	5.44
Mangrove	95	40.06	30.31	25.72	0.25	2.05

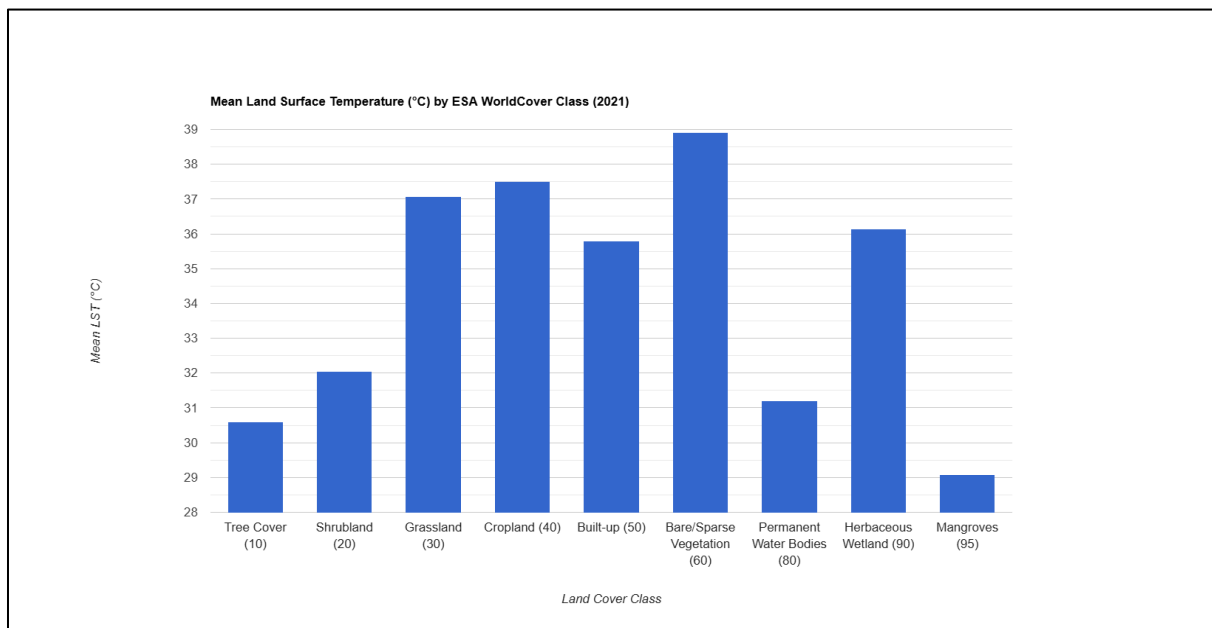


Figure 4.5: Mean LST for dry season across various LULC, 2021

Table 4.6: Mean, minimum and maximum NDVI for dry season, 2021

Land Cover	Dn	Max	Mean	Min	Area (%)	StdDev
Tree	10	0.43	0.27	0.01	7.38	0.05
Shrub	20	0.42	0.25	0.01	6.58	0.04
Grass	30	0.41	0.18	-0.05	43.58	0.04
Cropland	40	0.41	0.19	-0.04	10.02	0.04
Built up	50	0.38	0.12	-0.06	25.80	0.04
Bare	60	0.34	0.08	-0.11	2.00	0.03
Water	80	0.35	0.02	-0.14	2.25	0.04
Flooded vegetation	90	0.39	0.12	-0.09	2.14	0.08
Mangrove	95	0.38	0.17	-0.01	0.25	0.05

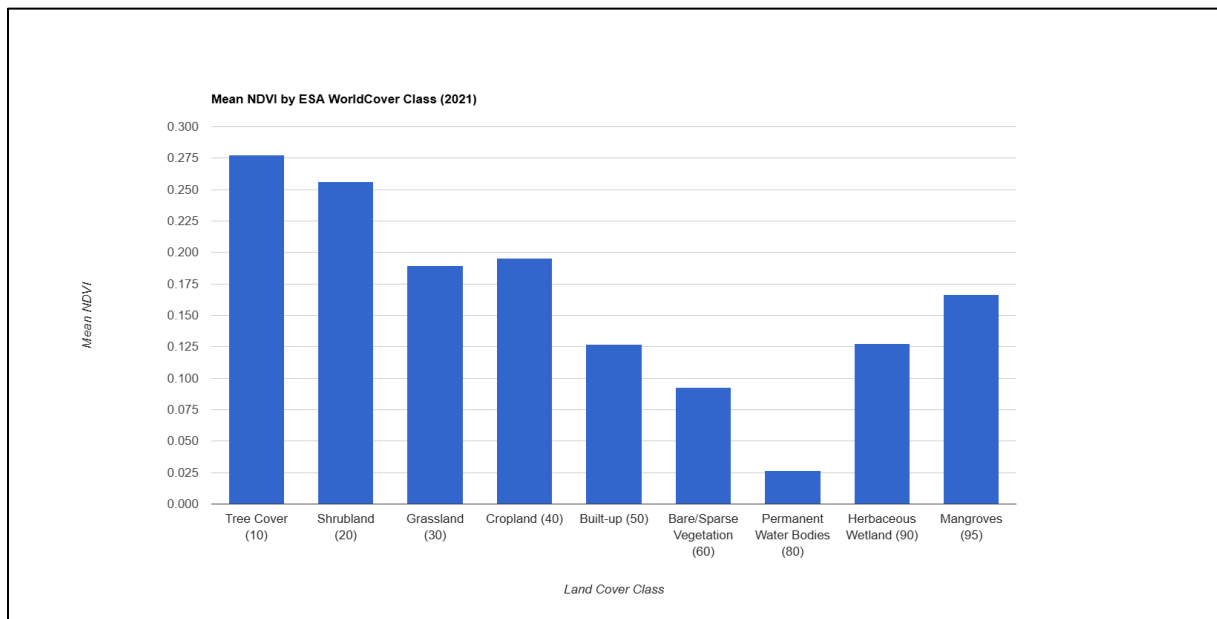


Figure 4.6: Mean LST for dry season across various LULC, 2021

4.3. Cooling Potential of Green Spaces

Mean LST in non-vegetation area is 37.30°C and that of vegetation area is 33.32°C and the cooling potential obtained is 3.98°C. This means green spaces (NDVI \geq 2.0), are on average 4 cooler than non-vegetation areas. LST range of vegetation areas is 24.67°C - 43.37°C and that of non-vegetation areas is 26.22°C - 43.36°C. The visualized map shows massive green spaces in the north with only patches of green within the built-up areas while the southern portion is dominated by non-vegetation. Notable green spaces within more dense impervious areas are the Achimota Forest, which is a government reserved forest within the heart of the region, and Legon Botanical Gardens.

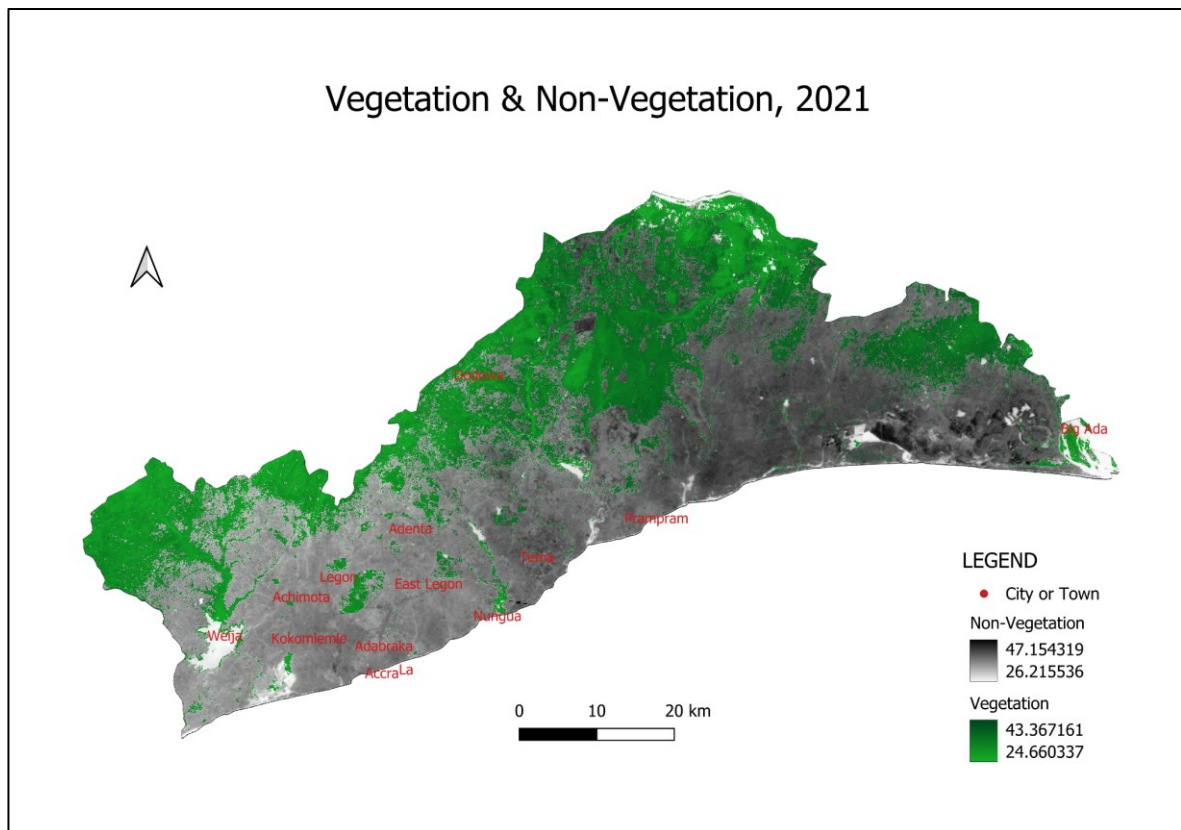


Figure 4.7: Showing Areas of Green and Non-Green Spaces

4.4. Cooling Intensity of UGSs

The line graph shows the cooling potential of each UGSs. Each of the five UGSs produced different cooling intensities and this is due various factors including the size, the height and thickness of vegetation, and microclimate of the surrounding (Jaganmohan et al., 2016; Y. Li et al., 2024). Legon and Achimota exhibit the highest cooling potential. Legon peaks at 4.1°C while Achimota peaks 3.3°C and flatten onwards from around 550m. These two well performing UGSs are the largest of the group which resonates with previous finds by (Yuan et al., 2018) Awudome and Osu Cemeteries perform moderately with about 2.5°C of cooling intensity around 180m indicating the limited influence of these green areas on nearby climate. Disperse vegetation and high built-up surroundings account for the low performance of these two green spaces. Similarly, Efua Sutherland Childrens’ Park showed extremely low potential mainly because of its small size and presence of high-rise buildings. This is an indication of urban heat interference on small vegetation which conforms with findings by Sheng et al (2025).

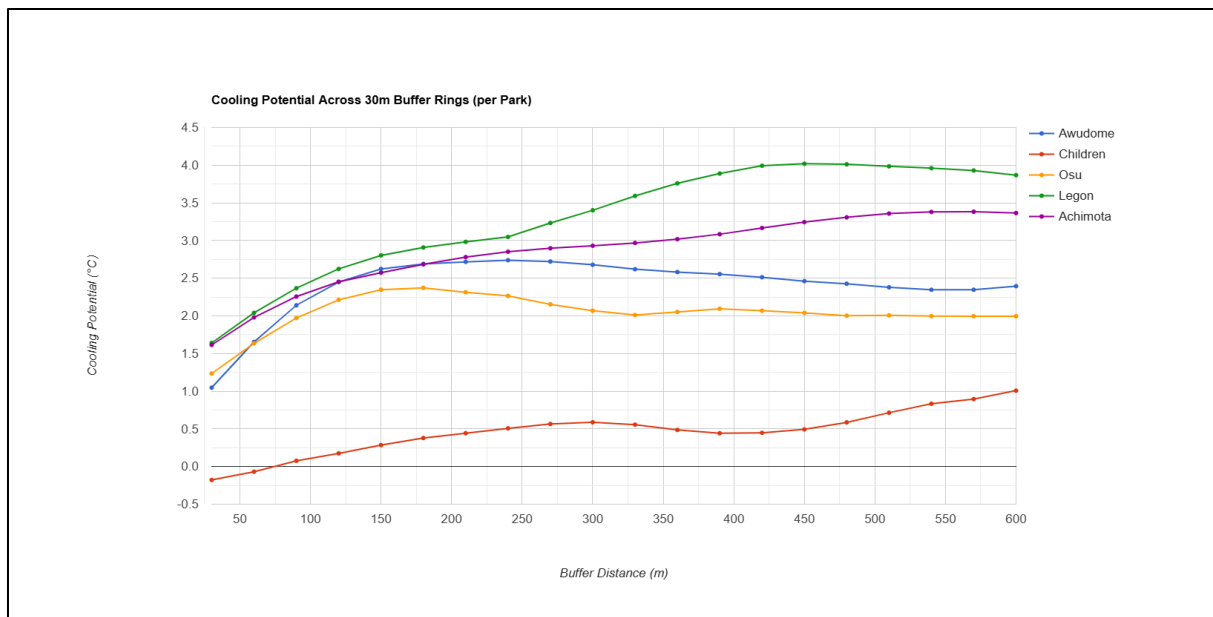


Figure 4.8: Cooling Potential Across 30m Buffer Rings (per Park)

4.4. Regression Analysis

The scatter plot shows a correlation between NDVI and LST using a sampled dataset. The regression model shows a fitted line with an equation shown below:

$$Y = -36.05x + 40.65$$

where y represents LST (°C) and x represents NDVI

The negative slope indicates inverse correlation between NDVI and LST, consistent with similar findings from several other studies (Chandrakar & Kumar Sinha, 2021; Devendran & Banon, 2023; Gelata et al., 2023). The coefficient of determination (R^2) is **0.57**, meaning **57% of the variance** in LST can be explained by variations in NDVI, a moderately strong relationship. A p-value of nearly 0 indicates a statistically high significant confirmation of the observed correlation. Higher NDVI values show denser vegetation which reduce LST due to evapotranspiration and shading compared to low NDVI values which represent bare, impervious surfaces or less vegetation areas where LST values are higher due to high heat retention of such surfaces. This conclusion is consistent with urban heat island effect (Chanpichaigosol et al., 2025)

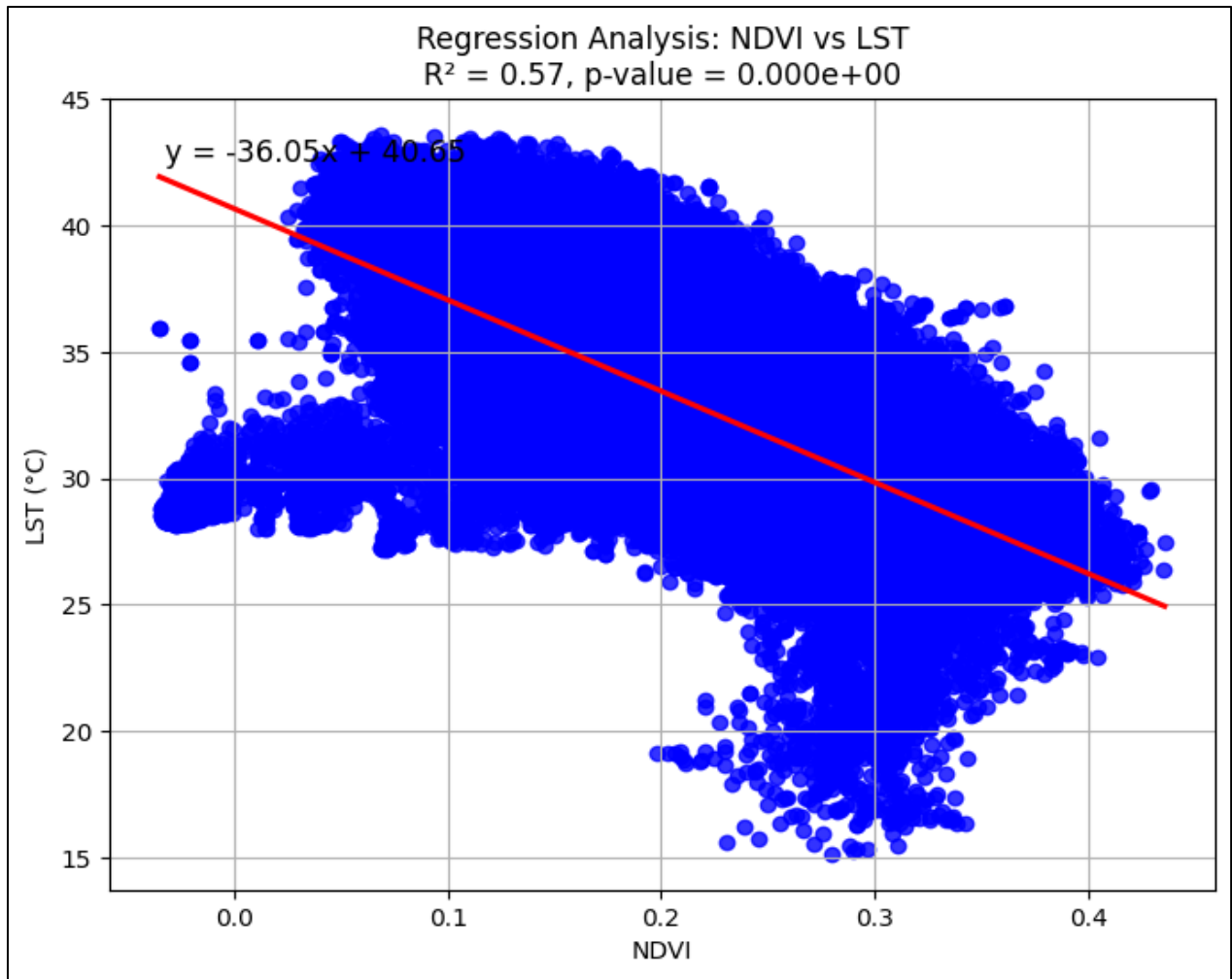


Figure 4.9: Graph of LST and NDVI

4.5. Scenarios

4.5.1. Urbanization vs Greening

The two scenarios being considered showed varying Mean LST values. Reducing grassland cover primarily due to urbanization and building of more impervious surfaces to 80% of grassland cover rises mean LST from 34.21°C to 35.0°C. This shows a warming of about 0.8°C. On the contrary, planting of trees to cover grassland by 80% reduces the mean LST of the 2021 dry season from 34.21°C to 33.13°C, indicating cooling of about 1.07°C. This has been shown spatially in figure 4.10.

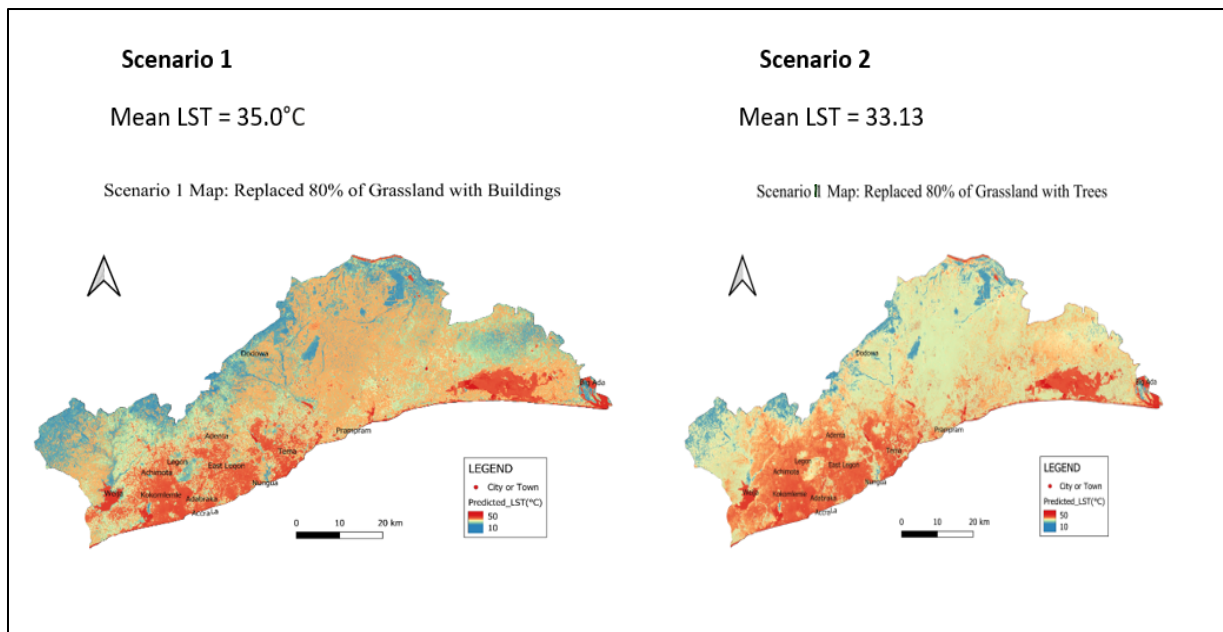


Figure 4.10: Figure showing the spatial changes in afforestation scenario against built-up

4.5.2. Shared Socio-economic Pathways

Currently, the heat stress index is estimated between 7.8 indicating a very high impact of heat on the human body. This is expected to rise further under various SSP scenarios. Except for the sustainability pathway (SSP1-/RCP2.6) which shows relatively lower projections for the year 2030, 2040 2050 and 2100, all pathways indicate extremely high indexes ranging from 7.9 to 8.3.

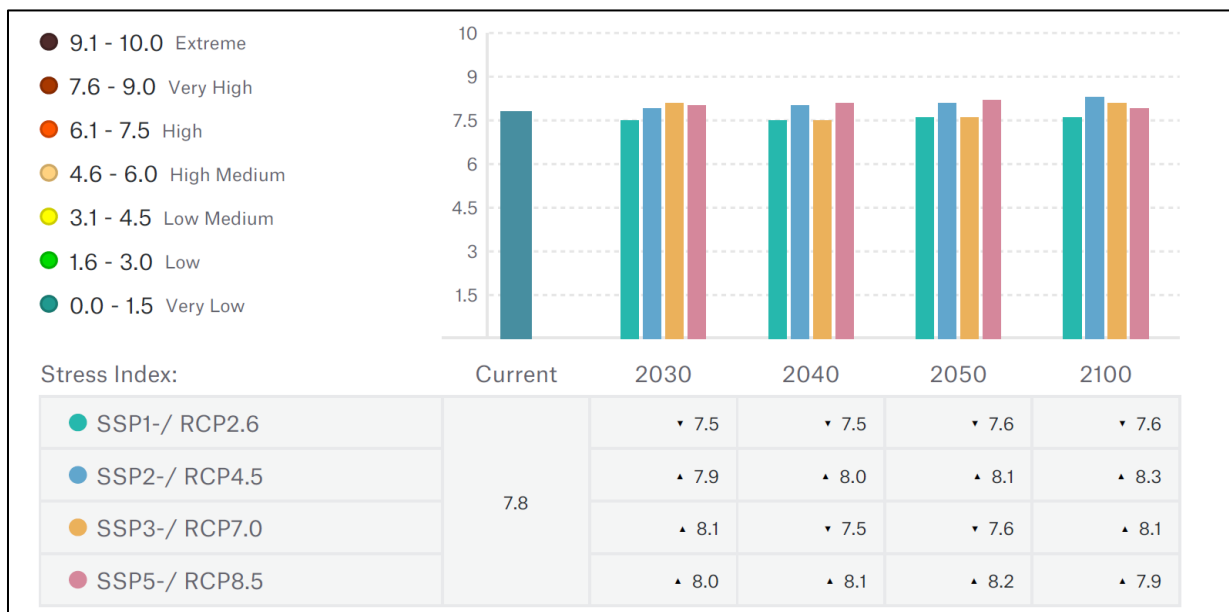


Figure 4.11: Shared Socio-Economic Pathway

4.6. DISCUSSION

The World Cover and Dynamic World datasets performed exceptionally well. Both products gave almost identical real-time value classification results. However, ESA World Cover had a significantly higher total accuracy of 99.85% than Dynamic World (70.96%). Both models are appropriate for their intended function, as they both received good accuracy ratings. The spatial resolution of both products is 10m, which is sufficient for our investigation. Dynamic World provides more frequently updated datasets than World Cover Map, making the former more dependable for short-term investigations. However, for the purpose of our study we would utilize ESA world cover because of its nearly perfect performance in classification assessment of our study area, this conforms to similar result shown in a study by Venter et al. in (2022)

Spatio-temporal analysis showed variation in LST with pronounced UHI in highly built-up areas such as Accra, Adabraka, Nungua, Tema, and Prampram. On the contrary, areas such as Weija, Legon, Achimota and Dodowa showed relatively lower LST due to high NDVI and tree cover. Over the years, however, LST and NDVI were found to be increasing and decreasing respectively due to increase in built-up areas and loss of green cover. The increasing LST and concurrent reducing NDVI over the period provides evidence of urban sprawl and receding tree cover in the Greater Accra region as evident in a study conducted by Devendran & Banon (2022).

Through a rigorous zonal analysis, it was proved that land covered with green cover such as trees, mangrove and shrubs show lower LST. This analysis provided an in-depth understanding to how various land cover across the study relate with LST and hence their cooling potential to reduce temperature. Tree cover had a momentous 5.44°C lower LST than built-up area. On the whole, green spaces in Greater Accra showed a cooling potential of about 4°C compared to non-green areas supported by observations made by Gyile et al. (2025)

A simple regression model shows a strong negative correlation between LST and NDVI justifying the cooling potential of vegetation as demonstrated in many studies (Massaro et al., 2023; Schwaab et al., 2021). This proves the significance of NDVI, which is an index of green cover, in mitigating LST and hence UHI resonating with recent findings by Gyile et al in 2025. Using the model, we have been able to estimate the minimum greenness to reduce LST and this is essential for policy and afforestation programs.

High thermal differences exist between the vegetation and non-vegetation areas. All parks except the Childrens' Park indicate an initial increase in cooling potential up to at least 300m which is consistent with previous findings in similar studies(Spronken-Smith & Oke, 1998). Cooling range is higher in Legon Botanical Garden followed by Achimota and almost non-existent around the Childrens' Park. While Achimota Forest is five-fold the size of Legon Botanical Garden, the latter shows the highest cooling intensity and cooling range among the five UGSs. This could be attributed to fragmentation within the Achimota Forest compared to Legon Botanical Garden (Jaganmohan et al., 2016). Also, in Legon, there are less impervious spaces in the surrounding built up areas and UHI is less pronounced compared to Achimota.

Using scenario analysis, it was observed that 80% of grassland converted to vegetation with at least vegetation index (NDVI) of 0.27 achieves a 1°C reduction in LST (using records of 2021). This is based on a huge assumption that all other factors remain constant.

Extremely high projected heat stress (7.5 - 8.3) under various SSPs scenarios is in conformation with other estimation studies (Vargas Zeppetello et al., 2022) which stated that for the tropics, the heat index will increase by 50 - 100 percent even when global warming is reduced below the thresholds (2°C) of the Paris Agreement.

5. CONCLUSION AND RECOMMENDATION

5.1. Conclusion

Green spaces play an important role in reducing LST, and hence they are essential in mitigating urban heat effects and improving quality of life. The effectiveness of urban greening scenarios in reducing extreme LST is significant. This goes to affirm the need for enhancing urban green spaces in urban development in the Greater Accra Region.

While green spaces have a significant cooling potential, urban green parks across the region remain fragmented making their cooling potential highly inefficient, calling for a more well-structured and incorporation of green spaces in urban restructuring and planning. The region lacks green spaces healthy enough to reduce LST during the dry season.

The result of scenario building has shown significance of adding more green infrastructure such as green roof, trees to urban built-up and reducing the cutting of trees. Policy implementation is a key to ensuring that our urban areas remain green, protect existing trees and mitigate urban heat. Accra must develop and implement frameworks like the Sydney Green Grid and Greener Places Framework to establish networks of green cover and open spaces in the city. Also, public education is also important to improve green space preservation and improving the incorporation of trees and other green facilities in homes. Increasing awareness among stakeholders and the general public about the value of urban green spaces, the importance of planting trees in our communities and protecting existing ones is crucial for sustainable urban living.

From the study trees, shrub and mangrove have shown to have the best option for reducing LST across the region, emphasizing the importance of afforestation and preservation of these species. When the rate of urbanization, loss of green space, and rate deforestation outstrip the rate afforestation, it will lead to extreme UHI effect, posing health risk to dwellers in certain areas of the region.

High cooling intensity proves a strong correlation between buffer distance and cooling potential. This is an indication of the significant role of well-placed and well sized UGSs in mitigating urban heat. Medium to large parks such as Achimota and Legon Botanical Garden serve as examples of well serving UGSs while smaller parks the Children's Park require

attention. The buffer analysis has proven to be a robust tool for estimating the spatial cooling gradients around UGSs. However, using surface temperature could be problematic as it does not exactly reflect the thermal situation on human skin (Martilli et al., 2020; Voogt & Oke, 2003).

Scenario analysis indicates extremely dangerous heat stress with associated health implications for humans under all SSP pathways, further amplifying the need to build more green spaces across the Greater Accra Region in face of increasing global warming and climate change.

5.2. Recommendation

Observed cooling efficiency of UGSs reinforces the need for large well vegetated green spaces in urban areas.

This study focused on one season and could not give a general perspective of the LST of the study area. Using Landsat data from December does not provide enough data to make a general conclusion. Using machine learning to harness insight from a large data set would be more reliable.

While NDVI is a valuable tool for comparing vegetation across urban areas, its numerical values do not indicate a direct relationship with physical quantities like biomass or weather parameters like temperature. As a result, analysing the NDVI values alone could be problematic and ambiguous. This limits the depth of the analysis and its application in urban planning and climate mitigation. For this reason, AGB can be employed in a future study.

This study focused on LST across the Greater Accra Region but this may be limiting. Using LST may not fully represent the thermal experience of people living in the region as it measures the temperature at the surface level. It is recommended to use multiple air temperature data collected across the region in order to correctly understand the impact of green spaces in face of increasing global temperatures.

Lastly, it is recommended that policy makers, the public and scientific communities build synergy towards a collaborative response to degradation and disregard of green spaces. It is worthy to note that urban green spaces are known to enhance communal engagement, promote peace coexistence and social interaction. As green spaces enhance the aesthetic appeal and attractiveness of neighbourhoods, it is the best interest of people to plant more trees.

6. REFERENCES

- Addi, M., Asare, K., Fosuhene, S. K., Ansah-Narh, T., Aidoo, K., & Botchway, C. G. (2021). Impact of Large-Scale Climate Indices on Meteorological Drought of Coastal Ghana. *Advances in Meteorology*, 2021, 1–17. <https://doi.org/10.1155/2021/8899645>
- Adom, R. K., Reid, M., Afuye, G. A., & Simatele, M. D. (2024). Assessing the Implications of Deforestation and Climate Change on Rural Livelihood in Ghana: A Multidimensional Analysis and Solution-Based Approach. *Environmental Management*, 74(6), 1124–1144. <https://doi.org/10.1007/s00267-024-02053-6>
- Adyatma, S., Muhaimin, M., Arisanty, D., & Hastuti, K. P. (2022). The Effect of Built-Up Area Density and Vegetation Density on Surface Temperature in Banjarmasin City. *International Journal of Forestry Research*, 2022, 1–12. <https://doi.org/10.1155/2022/2585719>
- Ahmed, H. A., Singh, S. K., Kumar, M., Maina, M. S., Dzwairo, R., & Lal, D. (2020). Impact of urbanization and land cover change on urban climate: Case study of Nigeria. *Urban Climate*, 32, 100600. <https://doi.org/10.1016/j.uclim.2020.100600>
- Alegria, C. (2023). Aboveground Biomass Mapping and Fire Potential Severity Assessment: A Case Study for Eucalypts <https://doi.org/10.3390/f14091795>
- Amekudzi, L., Yamba, E., Preko, K., Asare, E., Aryee, J., Baidu, M., & Codjoe, S. (2015). Variabilities in Rainfall Onset, Cessation and Length of Rainy Season for the Various Agro-Ecological Zones of Ghana. *Climate*, 3(2), 416–434. <https://doi.org/10.3390/cli3020416>
- Andrade, C., Fonseca, A., & Santos, J. A. (2023). Climate Change Trends for the Urban Heat Island Intensities in Two Major Portuguese Cities. *Sustainability*, 15(5), 3970. <https://doi.org/10.3390/su15053970>

- Aram, F., Higuera García, E., Solgi, E., & Mansournia, S. (2019). Urban green space cooling effect in cities. *Heliyon*, 5(4), e01339. <https://doi.org/10.1016/j.heliyon.2019.e01339>
- Asare, A., Boye, C. B., & Baffoe, P. E. (2024). Nexus Between Land Surface Temperature and Normalized Difference Vegetation Index in the Bole District in Ghana. *International Journal of Research and Scientific Innovation*, XI(VII), 849–862. <https://doi.org/10.51244/IJRSI.2024.1107067>
- Awotwi, A., Anornu, G. K., Quaye-Ballard, J. A., Annor, T., Forkuo, E. K., Harris, E., Agyekum, J., & Terlabie, J. L. (2019). Water balance responses to land-use/land-cover changes in the Pra River Basin of Ghana, 1986–2025. *CATENA*, 182, 104129. <https://doi.org/10.1016/j.catena.2019.104129>
- Awuni, S., Adarkwah, F., Ofori, B. D., Purwestri, R. C., Huertas Bernal, D. C., & Hajek, M. (2023). Managing the challenges of climate change mitigation and adaptation strategies in Ghana. *Heliyon*, 9(5). <https://doi.org/10.1016/j.heliyon.2023.e15491>
- Beltramone, G., Faustinelli, L. V., Pons, D., Bandini, M., Bressan, M. B., & Ferral, A. (2023, November). Comparison between Air Temperature and different Land Surface Temperature satellite products for the City of Córdoba, Argentina. In 2023 XX Workshop on Information Processing and Control (RPIC) (pp. 1-6). IEEE.
- Bevacqua, E., Schleussner, C.-F., & Zscheischler, J. (2025). A year above 1.5 °C signals that Earth is most probably within the 20-year period that will reach the Paris Agreement limit. *Nature Climate Change*, 15(3), 262–265. <https://doi.org/10.1038/s41558-025-02246-9>
- Borsah, A. A., Boah, E. A., & Brantson, E. T. (2025). Spatio-temporal land use/land cover change analysis and assessment of urban heat island in Ghana: A focus on the Greater Accra Region. *Journal of African Earth Sciences*, 221, 105474. <https://doi.org/10.1016/j.jafrearsci.2024.105474>

- Bowler, D. E., Buyung-Ali, L., Knight, T. M., & Pullin, A. S. (2010). Urban greening to cool towns and cities: A systematic review of the empirical evidence. *Landscape and Urban Planning*, 97(3), 147–155. <https://doi.org/10.1016/j.landurbplan.2010.05.006>
- Braimah, M., Asante, V. A., Ahiataku, M., Ansah, S. O., Otu-Larbi, F., Yahaya, B., & Ayabila, J. B. (2021). Seasonal Rainfall Variability over Southern Ghana. <https://doi.org/10.20944/preprints202108.0150.v1>
- Budiyanti, R. B. (2015). Measuring Ecological Values of Green Open Space Using Normalized Difference Vegetation Index Parameter. *Applied Mechanics and Materials*, 747, 101–104. <https://doi.org/10.4028/www.scientific.net/AMM.747.101>
- Calvin, K., Dasgupta, D., Krinner, G., Mukherji, A., Thorne, P. W., Trisos, C., Romero, J., Aldunce, P., Barrett, K., Blanco, G., Cheung, W. W. L., Connors, S., Denton, F., Diongue-Niang, A., Dodman, D., Garschagen, M., Geden, O., Hayward, B., Jones, C., ... Péan, C. (2023). IPCC, 2023: Climate Change 2023: Synthesis Report. Contribution of Working Groups I, II and III to the Sixth Assessment Report of the Intergovernmental Panel on Climate Change [Core Writing Team, H. Lee and J. Romero (eds.)]. IPCC, Geneva, Switzerland. (First). Intergovernmental Panel on Climate Change (IPCC). <https://doi.org/10.59327/IPCC/AR6-9789291691647>
- Chander, G., Markham, B. L., & Helder, D. L. (2009). Summary of current radiometric calibration coefficients for Landsat MSS, TM, ETM+, and EO-1 ALI sensors. *Remote Sensing of Environment*, 113(5), 893–903. <https://doi.org/10.1016/j.rse.2009.01.007>
- Chandrakar, S., & Kumar Sinha, M. (2021). 9 Comparative analysis of NDVI and LST to identify Urban Heat Island effect using remote sensing and GIS. In V. Dubey, S. R. K. Mishra, M. Michalska-Domańska, & V. Deshpande (Eds.), *Water Resource Technology* (pp. 99–110). De Gruyter. <https://doi.org/10.1515/9783110721355-009>
- Chang, C.-R., Li, M.-H., & Chang, S.-D. (2007). A preliminary study on the local cool-island

- intensity of Taipei city parks. *Landscape and Urban Planning*, 80(4), 386–395.
<https://doi.org/10.1016/j.landurbplan.2006.09.005>
- Chanpichaigosol, N., Chaichana, C., & Rinchumphu, D. (2025). Urban heat island classification through alternative normalized difference vegetation index. *Global Journal of Environmental Science and Management*, 11(1).
<https://doi.org/10.22034/gjesm.2025.01.04>
- Chunming, H., Shuaiqi, L., & Xi, D. (2024). A new method for evaluating the cold island effect in cities. *Urban Climate*, 54, 101846. <https://doi.org/10.1016/j.uclim.2024.101846>
- Damte, E., Manteaw, B. O., & Wrigley-Asante, C. (2023). Urbanization, climate change and health vulnerabilities in slum communities in Ghana. *The Journal of Climate Change and Health*, 10, 100189. <https://doi.org/10.1016/j.joclim.2022.100189>
- Devendran, A. A., & Banon, F. (2022). Spatio-Temporal Land Cover Analysis and the Impact of Land Cover Variability Indices on Land Surface Temperature in Greater Accra, Ghana Using Multi-Temporal Landsat Data. *Journal of Geographic Information System*, 14(03), 240–258. <https://doi.org/10.4236/jgis.2022.143013>
- Devendran, A. A., & Banon, F. (2023). Impact of Land Cover Variability Indices on Land Surface Temperature Using Multi-Temporal Landsat Data in Greater Accra, Ghana. In Dr. K. F. A. Lo (Ed.), *Novel Perspectives of Geography, Environment and Earth Sciences Vol. 3* (pp. 123–145). B P International (a part of SCIENCEDOMAIN International). <https://doi.org/10.9734/bpi/npgees/v3/4119C>
- Dissanayake, D., Morimoto, T., Murayama, Y., & Ranagalage, M. (2019). Impact of Landscape Structure on the Variation of Land Surface Temperature in Sub-Saharan Region: A Case Study of Addis Ababa using Landsat Data (1986–2016). *Sustainability*, 11(8), 2257. <https://doi.org/10.3390/su11082257>
- Duarte, D., Fonte, C., Costa, H., & Caetano, M. (2023). Thematic Comparison between ESA

- WorldCover 2020 Land Cover Product and a National Land Use Land Cover Map. *Land*, 12(2), 490. <https://doi.org/10.3390/land12020490>
- Estoque, R. C., Murayama, Y., & Myint, S. W. (2017). Effects of landscape composition and pattern on land surface temperature: An urban heat island study in the megacities of Southeast Asia. *Science of The Total Environment*, 577, 349–359. <https://doi.org/10.1016/j.scitotenv.2016.10.195>
- Ferral, A., Gili, A., Andreo, V., German, A., Beltramone, G., Bonansea, M., ... & Scavuzzo, M. (2021, November). Calculation of surface urban heat index from LANDSAT-8 TIRS data and its relation with land cover. In 2021 XIX Workshop on Information Processing and Control (RPIC) (pp. 1-6). IEEE.
- Feyisa, G. L., Dons, K., & Meilby, H. (2014). Efficiency of parks in mitigating urban heat island effect: An example from Addis Ababa. *Landscape and Urban Planning*, 123, 87–95. <https://doi.org/10.1016/j.landurbplan.2013.12.008>
- Frimpong, B. F., Koranteng, A., & Opoku, F. S. (2023). Analysis of urban expansion and its impact on temperature utilising remote sensing and GIS techniques in the Accra Metropolis in Ghana (1986–2022). *SN Applied Sciences*, 5(8), 225. <https://doi.org/10.1007/s42452-023-05439-z>
- Gelata, F. T., Jiqin, H., Chaka Gameda, S., & Wubishet Asefa, B. (2023). Application of GIS using NDVI and LST estimation to measure climate variability-induced drought risk assessment in Ethiopia. *Journal of Water and Climate Change*, 14(7), 2479–2489. <https://doi.org/10.2166/wcc.2023.154>
- Global climate change. (n.d.). [dataset]. <https://doi.org/10.1036/1097-8542.757541>
- Grilo, F., Pinho, P., Aleixo, C., Catita, C., Silva, P., Lopes, N., Freitas, C., Santos-Reis, M., McPhearson, T., & Branquinho, C. (2020). Using green to cool the grey: Modeling the cooling effect of green spaces with a high spatial resolution. *Science of The Total*

- Environment, 724, 138182. <https://doi.org/10.1016/j.scitotenv.2020.138182>
- Guha, S., & Govil, H. (2021). COVID-19 lockdown effect on land surface temperature and normalized difference vegetation index. *Geomatics, Natural Hazards and Risk*, 12(1), 1082–1100. <https://doi.org/10.1080/19475705.2021.1914197>
- Gyasi-Addo, J. (2021). Evaluation of the effect of urbanization on urban thermal behaviour using urban heat island indicators: The case of the CBD of Accra [Robert Gordon University; PDF]. <https://doi.org/10.48526/RGU-WT-1603337>
- Gyasi-Addo, J. (2021). Evaluation of the effect of urbanization on urban thermal behaviour using urban heat island indicators: The case of the CBD of Accra [Robert Gordon University; PDF]. <https://doi.org/10.48526/RGU-WT-1603337>
- Gyile, D. N., Asare, A., Osei-Gyabaah, A. P., & Anaafo, D. (2025). Assessment of Land Use and Land Cover Changes and Their Impact on Land Surface Temperature in Greater Accra, Ghana. <https://doi.org/10.2139/ssrn.5077196>
- Gyimah, R. R., Kwang, C., Antwi, R. A., Morgan Attua, E., Owusu, A. B., & Doe, E. K. (2023). Trading greens for heated surfaces: Land surface temperature and perceived health risk in Greater Accra Metropolitan Area, Ghana. *The Egyptian Journal of Remote Sensing and Space Sciences*, 26(4), 861–880. <https://doi.org/10.1016/j.ejrs.2023.09.004>
- Hsu, A., Sheriff, G., Chakraborty, T., & Manya, D. (2021). Disproportionate exposure to urban heat island intensity across major US cities. *Nature Communications*, 12(1), 2721. <https://doi.org/10.1038/s41467-021-22799-5>
- Huang, S., Tang, L., Hupy, J. P., Wang, Y., & Shao, G. (2021). A commentary review on the use of normalized difference vegetation index (NDVI) in the era of popular remote sensing. *Journal of Forestry Research*, 32(1), 1–6. <https://doi.org/10.1007/s11676-020-01155-1>
- Jaganmohan, M., Knapp, S., Buchmann, C. M., & Schwarz, N. (2016). The Bigger, the Better?

- The Influence of Urban Green Space Design on Cooling Effects for Residential Areas. *Journal of Environmental Quality*, 45(1), 134–145. <https://doi.org/10.2134/jeq2015.01.0062>
- Jimenez-Munoz, J. C., Sobrino, J. A., Skokovic, D., Mattar, C., & Cristobal, J. (2014). Land Surface Temperature Retrieval Methods from Landsat-8 Thermal Infrared Sensor Data. *IEEE Geoscience and Remote Sensing Letters*, 11(10), 1840–1843. <https://doi.org/10.1109/LGRS.2014.2312032>
- Kabisch, N., Remahne, F., Ilsemann, C., & Fricke, L. (2023). The urban heat island under extreme heat conditions: A case study of Hannover, Germany. *Scientific Reports*, 13(1), 23017. <https://doi.org/10.1038/s41598-023-49058-5>
- Kanjin, K., & Alam, B. M. (2024). Assessing changes in land cover, NDVI, and LST in the Sundarbans mangrove forest in Bangladesh and India: A GIS and remote sensing approach. *Remote Sensing Applications: Society and Environment*, 36, 101289. <https://doi.org/10.1016/j.rsase.2024.101289>
- Kelsey, K., & Neff, J. (2014). Estimates of Aboveground Biomass from Texture Analysis of Landsat Imagery. *Remote Sensing*, 6(7), 6407–6422. <https://doi.org/10.3390/rs6076407>
- Kotir, C., Amponsah, O., Anbazu, J., Takyi, S. A., Blija, D. K., & Frempong, F. (2024). Unveiling Ghana's urban tapestry: Satellite-based analysis of Tamale city's spatial expansion and land surface temperature (LST) dynamics. *GeoJournal*, 89(6), 242. <https://doi.org/10.1007/s10708-024-11243-y>
- Kwofie, S., Nyamekye, C., Appiah Boamah, L., Owusu Adjei, F., Arthur, R., & Agyapong, E. (2022). Urban growth nexus to land surface temperature in Ghana. *Cogent Engineering*, 9(1), 2143045. <https://doi.org/10.1080/23311916.2022.2143045>
- Lanzante, J. R. (2024). A New Heat Stress Index for Climate Change Assessment. *Bulletin of the American Meteorological Society*, 105(12), E2482–E2495.

<https://doi.org/10.1175/BAMS-D-24-0030.1>

- Li, D., Wu, S., Liang, Z., & Li, S. (2020). The impacts of urbanization and climate change on urban vegetation dynamics in China. *Urban Forestry & Urban Greening*, 54, 126764. <https://doi.org/10.1016/j.ufug.2020.126764>
- Li, J., Song, C., Cao, L., Zhu, F., Meng, X., & Wu, J. (2011). Impacts of landscape structure on surface urban heat islands: A case study of Shanghai, China. *Remote Sensing of Environment*, 115(12), 3249–3263. <https://doi.org/10.1016/j.rse.2011.07.008>
- Li, L., Zhan, W., Hu, L., Chakraborty, T., Wang, Z., Fu, P., Wang, D., Liao, W., Huang, F., Fu, H., Li, J., Liu, Z., Du, H., & Wang, S. (2023). Divergent urbanization-induced impacts on global surface urban heat island trends since 1980s. *Remote Sensing of Environment*, 295, 113650. <https://doi.org/10.1016/j.rse.2023.113650>
- Li, Y., Svenning, J.-C., Zhou, W., Zhu, K., Abrams, J. F., Lenton, T. M., Ripple, W. J., Yu, Z., Teng, S. N., Dunn, R. R., & Xu, C. (2024). Green spaces provide substantial but unequal urban cooling globally. *Nature Communications*, 15(1), 7108. <https://doi.org/10.1038/s41467-024-51355-0>
- Liu, J., Varghese, B. M., Hansen, A., Zhang, Y., Driscoll, T., Morgan, G., Dear, K., Gourley, M., Capon, A., & Bi, P. (2022). Heat exposure and cardiovascular health outcomes: A systematic review and meta-analysis. *The Lancet Planetary Health*, 6(6), e484–e495. [https://doi.org/10.1016/S2542-5196\(22\)00117-6](https://doi.org/10.1016/S2542-5196(22)00117-6)
- Liu, W., Zhao, H., Sun, S., Xu, X., Huang, T., & Zhu, J. (2022). Green Space Cooling Effect and Contribution to Mitigate Heat Island Effect of Surrounding Communities in Beijing Metropolitan Area. *Frontiers in Public Health*, 10, 870403. <https://doi.org/10.3389/fpubh.2022.870403>
- Mandal, M., Popek, R., Przybysz, A., Roy, A., Das, S., & Sarkar, A. (2023). Breathing Fresh Air in the City: Implementing Avenue Trees as a Sustainable Solution to Reduce

- Particulate Pollution in Urban Agglomerations. *Plants*, 12(7), 1545.
<https://doi.org/10.3390/plants12071545>
- Mantey, S., Tagoe, N. D., & Abaidoo, C. A. (n.d.). Estimation of Land Surface Temperature and Vegetation Abundance Relationship – A Case Study.
- Manzanas, R., Amekudzi, L. K., Preko, K., Herrera, S., & Gutiérrez, J. M. (2014). Precipitation variability and trends in Ghana: An intercomparison of observational and reanalysis products. *Climatic Change*, 124(4), 805–819. <https://doi.org/10.1007/s10584-014-1100-9>
- Martilli, A., Krayenhoff, E. S., & Nazarian, N. (2020). Is the Urban Heat Island intensity relevant for heat mitigation studies? *Urban Climate*, 31, 100541.
<https://doi.org/10.1016/j.uclim.2019.100541>
- Martinez, A. D. L. I., & Labib, S. M. (2023). Demystifying normalized difference vegetation index (NDVI) for greenness exposure assessments and policy interventions in urban greening. *Environmental Research*, 220, 115155.
<https://doi.org/10.1016/j.envres.2022.115155>
- Massaro, E., Schifanella, R., Piccardo, M., Caporaso, L., Taubenböck, H., Cescatti, A., & Duveiller, G. (2023). Spatially-optimized urban greening for reduction of population exposure to land surface temperature extremes. *Nature Communications*, 14(1), 2903.
<https://doi.org/10.1038/s41467-023-38596-1>
- Meadows, J., Mansour, A., Gatto, M. R., Li, A., Howard, A., & Bentley, R. (2024). Mental illness and increased vulnerability to negative health effects from extreme heat events: A systematic review. *Psychiatry Research*, 332, 115678.
<https://doi.org/10.1016/j.psychres.2023.115678>
- Mitraka, Z., Chrysoulakis, N., Kamarianakis, Y., Partsinevelos, P., & Tsouchlaraki, A. (2012). Improving the estimation of urban surface emissivity based on sub-pixel classification

- of high-resolution satellite imagery. *Remote Sensing of Environment*, 117, 125–134.
<https://doi.org/10.1016/j.rse.2011.06.025>
- Morales-Barquero, L., Lyons, M., Phinn, S., & Roelfsema, C. (2019). Trends in Remote Sensing Accuracy Assessment Approaches in the Context of Natural Resources. *Remote Sensing*, 11(19), 2305. <https://doi.org/10.3390/rs11192305>
- Moss, R. H., Edmonds, J. A., Hibbard, K. A., Manning, M. R., Rose, S. K., Van Vuuren, D. P., Carter, T. R., Emori, S., Kainuma, M., Kram, T., Meehl, G. A., Mitchell, J. F. B., Nakicenovic, N., Riahi, K., Smith, S. J., Stouffer, R. J., Thomson, A. M., Weyant, J. P., & Wilbanks, T. J. (2010). The next generation of scenarios for climate change research and assessment. *Nature*, 463(7282), 747–756. <https://doi.org/10.1038/nature08823>
- O'Neill, B. C., Kriegler, E., Riahi, K., Ebi, K. L., Hallegatte, S., Carter, T. R., Mathur, R., & Van Vuuren, D. P. (2014). A new scenario framework for climate change research: The concept of shared socioeconomic pathways. *Climatic Change*, 122(3), 387–400.
<https://doi.org/10.1007/s10584-013-0905-2>
- Oliveira, S., Andrade, H., & Vaz, T. (2011). The cooling effect of green spaces as a contribution to the mitigation of urban heat: A case study in Lisbon. *Building and Environment*, 46(11), 2186–2194. <https://doi.org/10.1016/j.buildenv.2011.04.034>
- Olofsson, P., Foody, G. M., Herold, M., Stehman, S. V., Woodcock, C. E., & Wulder, M. A. (2014). Good practices for estimating area and assessing accuracy of land change. *Remote Sensing of Environment*, 148, 42–57. <https://doi.org/10.1016/j.rse.2014.02.015>
- Oppong, J., Namwamba, J. B., Twumasi, Y. A., Ning, Z. H., Asare-Ansah, A. B., Akinrinwoye, C., Antwi, R., Osimbo, B. M., Loh, P., Frimpong, D. B., Apraku, C., Atayi, J., Ahoma, G., & Annan, J. (2023). Urbanization and urban forest loss: A spatial analysis of five metropolitan districts in Ghana. *Geology, Ecology, and Landscapes*, 1–10.
<https://doi.org/10.1080/24749508.2023.2202439>

- Osei, M. A., Amekudzi, L. K., & Quansah, E. (2021). Characterisation of wet and dry spells and associated atmospheric dynamics at the Pra River catchment of Ghana, West Africa. *Journal of Hydrology: Regional Studies*, 34, 100801. <https://doi.org/10.1016/j.ejrh.2021.100801>
- Owusu, A. B. (2018). An Assessment of Urban Vegetation Abundance in Accra Metropolitan Area, Ghana: A Geospatial Approach. *Journal of Environmental Geography*, 11(1–2), 37–44. <https://doi.org/10.2478/jengeo-2018-0005>
- Peeters, A., Shashua-Bar, L., Meir, S., Shmulevich, R. R., Caspi, Y., Weyl, M., Motzafi-Haller, W., & Angel, N. (2020). A decision support tool for calculating effective shading in urban streets. *Urban Climate*, 34, 100672. <https://doi.org/10.1016/j.uclim.2020.100672>
- Peng, J., Dan, Y., Qiao, R., Liu, Y., Dong, J., & Wu, J. (2021). How to quantify the cooling effect of urban parks? Linking maximum and accumulation perspectives. *Remote Sensing of Environment*, 252, 112135. <https://doi.org/10.1016/j.rse.2020.112135>
- Peng, X., Wu, W., Zheng, Y., Sun, J., Hu, T., & Wang, P. (2020). Correlation analysis of land surface temperature and topographic elements in Hangzhou, China. *Scientific Reports*, 10(1), 10451. <https://doi.org/10.1038/s41598-020-67423-6>
- Perkins-Kirkpatrick, S. E., & Lewis, S. C. (2020). Increasing trends in regional heatwaves. *Nature Communications*, 11(1), 3357. <https://doi.org/10.1038/s41467-020-16970-7>
- Phan, T., Kappas, M., & Tran, T. (2018). Land Surface Temperature Variation Due to Changes in Elevation in Northwest Vietnam. *Climate*, 6(2), 28. <https://doi.org/10.3390/cli6020028>
- Rendana, M., Razi Idris, W. M., Abdul Rahim, S., Ghassan Abdo, H., Almohamad, H., Abdullah Al Dughairi, A., & Albanai, J. A. (2023). Effects of the built-up index and land surface temperature on the mangrove area change along the southern Sumatra coast. *Forest Science and Technology*, 19(3), 179–189.

<https://doi.org/10.1080/21580103.2023.2220576>

- Schwaab, J., Meier, R., Mussetti, G., Seneviratne, S., Bürgi, C., & Davin, E. L. (2021). The role of urban trees in reducing land surface temperatures in European cities. *Nature Communications*, 12(1), 6763.
- Sekertekin, A., & Bonafoni, S. (2020). Land Surface Temperature Retrieval from Landsat 5, 7, and 8 over Rural Areas: Assessment of Different Retrieval Algorithms and Emissivity Models and Toolbox Implementation. *Remote Sensing*, 12(2), 294. <https://doi.org/10.3390/rs12020294>
- Shashua-Bar, L., Pearlmutter, D., & Erell, E. (2011). The influence of trees and grass on outdoor thermal comfort in a hot-arid environment. *International Journal of Climatology*, 31(10), 1498–1506. <https://doi.org/10.1002/joc.2177>
- Sheng, Q., Ji, Y., Jia, C., Jiang, L., Li, C., Huang, Z., Ma, C., Zhang, X., Chen, H., Wang, T., Zhu, Y., & Zhu, Z. (2025). Differential effects of cooling and humidification in urban green spaces and thresholds of vegetation community structure parameters: A case study of the Yangtze River Delta region. *Cities*, 159, 105765. <https://doi.org/10.1016/j.cities.2025.105765>
- Shi, T., Liu, L., Wen, X., & Qi, P. (2024). Research progress on the synergies between heat waves and canopy urban heat island and their driving factors. *Frontiers in Environmental Science*, 12, 1363837.
- Spronken-Smith, R. A., & Oke, T. R. (1998). The thermal regime of urban parks in two cities with different summer climates. *International Journal of Remote Sensing*, 19(11), 2085–2104. <https://doi.org/10.1080/014311698214884>
- Stow, D. A., Weeks, J. R., Toure, S., Coulter, L. L., Lippitt, C. D., & Ashcroft, E. (2013). Urban Vegetation Cover and Vegetation Change in Accra, Ghana: Connection to Housing Quality. *The Professional Geographer*, 65(3), 451–465.

<https://doi.org/10.1080/00330124.2012.697856>

Tong, S., Prior, J., McGregor, G., Shi, X., & Kinney, P. (2021). Urban heat: An increasing threat to global health. *BMJ*, n2467. <https://doi.org/10.1136/bmj.n2467>

Twumasi, Y. A., Merem, E. C., Namwamba, J. B., Mwakimi, O. S., Ayala-Silva, T., Frimpong, D. B., Ning, Z. H., Asare-Ansah, A. B., Annan, J. B., Oppong, J., Loh, P. M., Owusu, F., Jeruto, V., Petja, B. M., Okwemba, R., McClendon-Peralta, J., Akinrinwoye, C. O., & Mosby, H. J. (2021). Estimation of Land Surface Temperature from Landsat-8 OLI Thermal Infrared Satellite Data. A Comparative Analysis of Two Cities in Ghana. *Advances in Remote Sensing*, 10(04), 131–149. <https://doi.org/10.4236/ars.2021.104009>

Twumasi, Y. A., Merem, E. C., Namwamba, J. B., Mwakimi, O. S., Ayala-Silva, T., Frimpong, D. B., Ning, Z. H., Asare-Ansah, A. B., Annan, J. B., Oppong, J., Loh, P. M., Owusu, F., Jeruto, V., Petja, B. M., Okwemba, R., McClendon-Peralta, J., Akinrinwoye, C. O., & Mosby, H. J. (2021). Estimation of Land Surface Temperature from Landsat-8 OLI Thermal Infrared Satellite Data. A Comparative Analysis of Two Cities in Ghana. *Advances in Remote Sensing*, 10(04), 131–149. <https://doi.org/10.4236/ars.2021.104009>

Vargas Zeppetello, L. R., Raftery, A. E., & Battisti, D. S. (2022). Probabilistic projections of increased heat stress driven by climate change. *Communications Earth & Environment*, 3(1), 183. <https://doi.org/10.1038/s43247-022-00524-4>

Venter, Z. S., Barton, D. N., Chakraborty, T., Simensen, T., & Singh, G. (2022). Global 10 m Land Use Land Cover Datasets: A Comparison of Dynamic World, World Cover and Esri Land Cover. *Remote Sensing*, 14(16), 4101. <https://doi.org/10.3390/rs14164101>

Voogt, J. A., & Oke, T. R. (2003). Thermal remote sensing of urban climates. *Remote Sensing of Environment*, 86(3), 370–384. [https://doi.org/10.1016/S0034-4257\(03\)00079-8](https://doi.org/10.1016/S0034-4257(03)00079-8)

- Wang, R., Feng, Z., Pearce, J., Liu, Y., & Dong, G. (2021). Are greenspace quantity and quality associated with mental health through different mechanisms in Guangzhou, China: A comparison study using street view data. *Environmental Pollution*, 290, 117976. <https://doi.org/10.1016/j.envpol.2021.117976>
- Wemegah, C. S., Yamba, E. I., Aryee, J. N. A., Sam, F., & Amekudzi, L. K. (2020). Assessment of urban heat island warming in the greater accra region. *Scientific African*, 8, e00426. <https://doi.org/10.1016/j.sciaf.2020.e00426>
- Weng, Q. (2009). Thermal infrared remote sensing for urban climate and environmental studies: Methods, applications, and trends. *ISPRS Journal of Photogrammetry and Remote Sensing*, 64(4), 335–344. <https://doi.org/10.1016/j.isprsjprs.2009.03.007>
- Yang, J., Ren, J., Sun, D., Xiao, X., Xia, J. (Cecilia), Jin, C., & Li, X. (2021). Understanding land surface temperature impact factors based on local climate zones. *Sustainable Cities and Society*, 69, 102818. <https://doi.org/10.1016/j.scs.2021.102818>
- Yao, X., Yu, K., Zeng, X., Lin, Y., Ye, B., Shen, X., & Liu, J. (2022). How can urban parks be planned to mitigate urban heat island effect in “Furnace cities”? An accumulation perspective. *Journal of Cleaner Production*, 330, 129852. <https://doi.org/10.1016/j.jclepro.2021.129852>
- Yazdanie, M., Frimpong, P. B., Dramani, J. B., & Orehounig, K. (2024). The impacts of the informal economy, climate migration, and rising temperatures on energy system planning. *Energy Reports*, 11, 165–178. <https://doi.org/10.1016/j.egy.2023.11.041>
- Yu, Z., Guo, X., Jørgensen, G., & Vejre, H. (2017). How can urban green spaces be planned for climate adaptation in subtropical cities? *Ecological Indicators*, 82, 152–162. <https://doi.org/10.1016/j.ecolind.2017.07.002>
- Yuan, H., Wu, C., Lu, L., & Wang, X. (2018). A new algorithm predicting the end of growth at five evergreen conifer forests based on nighttime temperature and the enhanced

vegetation index. *ISPRS Journal of Photogrammetry and Remote Sensing*, 144, 390–399. <https://doi.org/10.1016/j.isprsjprs.2018.08.013>

Zhang, J., Zhang, H., & Qi, R. (2024). A study of size threshold for cooling effect in urban parks and their cooling accessibility and equity. *Scientific Reports*, 14(1), 16176. <https://doi.org/10.1038/s41598-024-67277-2>

Zhao, J., Zhao, X., Liang, S., Zhou, T., Du, X., Xu, P., & Wu, D. (2020). Assessing the thermal contributions of urban land cover types. *Landscape and Urban Planning*, 204, 103927. <https://doi.org/10.1016/j.landurbplan.2020.103927>